Department of Precision and Microsystems Engineering

Compliant curved beam transmission systems

R.F.L. Gerlach

Report no : 2021.050
Coaches : Dr. ir. G. Radaelli, & Ir. A. Amoozandeh Nobaveh
Professor : Prof. dr. ir. J.L. Herder
Specialisation : Mechatronic System Design
Type of report : Master thesis
Date : 30/07/2021

TU Delft

Challenge the future

Compliant curved beam transmission systems

by

R.F.L. Gerlach

to obtain the degree of Master of Science
at the Delft University of Technology,
to be defended publicly on Friday July 30, 2021 at 14:30.

Student number:	5173906	
Department:	Precision and Microsystems Engineering	
Specialisation:	Mechatronic System Design	
Thesis committee:	Prof. dr. ir. J.L. Herder,	TU Delft, supervisor
	Dr. ir. G. Radaelli,	TU Delft, daily supervisor
	Ir. A. Amoozandeh Nobaveh,	TU Delft, daily supervisor

This thesis is confidential and cannot be made public until August, 2023

TU Delft

Preface

"Nothing is absolute. Everything changes, everything moves, everything revolves, everything flies and goes away."
Frida Kahlo

The very first time I stepped into the Technical University of Delft to obtain information about their master programs I joined a lecture given by Just Herder about the High-Tech engineering track. I have heard about this phenomenon when the border between the application of advanced fundamental research and magic seems to disappear. That is what I felt like on that day, the day I got introduced to compliant mechanisms. One of the concepts that I remembered most was this two-dimensional round plate, not bigger than a coin which was able to replace fundamental parts of a mechanical watch. It seemed impossible to develop something that could replace gears, increase the accuracy and be much more efficient. How does this work? how can we tune this? and what are the possibilities for the future?

When I came across the possibility to work on a compliant mechanism for my thesis I was very excited. The first online meeting with Giuseppe and Ali was very inspirational and there seemed to be endless possibilities. I never lost these feelings during the year that followed. Something also that contributed to this, was the involvement of Laevo Exoskeletons. During the three months of internship that I have spent at Laevo, I received loads of professional support, creative freedom, and the possibility to physically create the ideas I had. Their R&D team showed me how people with different experiences can efficiently cooperate to develop a product that can make the everyday lives of many people a little better.

Due to the COVID- 19 situation, the last 1,5 years were anything but normal. For courses, there were great logistic problems as lectures and exams included too many students to facilitate on the university. The first improvised online exams were complete chaos but became much better already after the first period. Not only the courses but also doing a thesis became very different. I had never expected to spend so many hours in front of the camera, having group meetings or progress meetings on zoom. Luckily, when the measures allowed, there was also room to meet each other face to face at the university. Last week was the first time the whole group was together to have diner. It is always funny to see people in real life for the first time, for some reason, they always tend to be very different from your expectations. Overall I feel like the university offered support where needed and everybody involved showed great flexibility and creativity to handle the situation.

Almost two years ago I came to Delft aiming to obtain a master's degree in High-Tech Engineering from the technical university. This report holds the result of one year of knowledge obtained during lectures, and one year of research, symbolizing the final step of my journey. I hope anyone who reads it can enjoy it as much as I did.

R.F.L. Gerlach
Delft, Augustus 2021

Acknowledgements

Much of my appreciation for the people and organizations involved in this master thesis is already shown in the preface of this report. Nevertheless, I feel like some explicit notions of their support, facilities, and involvement should still be made.

First I would like to thank my thesis committee. Professor Just herder, Giuseppe, and Ali thank you all for the guidance throughout the year and the critical and honest feedback. Ali, thank you for your support, daily supervision, and the occasional pep talks when needed. The shell-skeletons group provided a great platform for me to have discussions with fellow students, have regular meetings, and ask for help when needed. Many of the students that graduated before me set a great example by providing guidelines throughout my project. I would like to thank all the students from the group, present now, but also those who already finished over the last year for being critical and being available for questions.

Secondly, I would like to show my appreciation for Laevo. During my internship as well as during the continuation of my master thesis I have enjoyed the support and discussions which I had with Bas, my main supervisor who guided this project. The whole R&D team at Laevo creates a working environment that is almost like you are part of the Laevo family. There is a lot of freedom within your project to make your own decisions and pursue your own path. Thank you all, Jaromir, Mike, Boudewijn, and Frank.

Lastly, but most importantly I would like to acknowledge the involvement of my friends and family. My roommates, who became my colleagues during these COVID-19 times keeping me company during lunch and coffee breaks. Tolerating me when I used the diner table as a workbench, cutting and gluing new prototypes. My friends, providing the necessary distraction and support during challenging times. I would like to thank my family, my mother, and my sister, who always supported me throughout my studies, even though I chose to become an engineer, a path not familiar to them. My extended family from Limburg, providing a safe and warm place for occasional trips. And finally, my boyfriend, empowering me in every decision I make to become who I am today.

Contents

1

Introduction

Passive exoskeletons have become more popular over the last couple of years. Not only in applications where they enhance abilities, but also in supporting abilities in order to prevent injuries. An example of an exoskeleton in this last category is the Laevo back support. The Laevo is developed for people within professions including physical activity, specifically heavy lifting, bending over and working in bend over positions. The system, exists out of 3 main components: a connection to the upper body, a connection to the lower body and a spring connecting the two. The spring, which is located on the hips, supports the lower back by providing an upwards moment. The moment, releases or reduces the tension in the lower back which results in less back problems over time. For the system to be of additional value, for most users it is important that it does not affect or aggravate other activities that do not concern bending or leaning over.

A challenging part of the kinematics of the design is the decoupling of the bending motion and a walking motion. Both load cases involve the angle between the upper and lower body to decrease, which puts the smart joints under tension. However, when walking, it is not desired to have an opposing moment from the smart joints pressing on your legs. This makes it more difficult to walk and significantly increases the amount of energy needed to do so. One of the manners to achieve the decoupling of these load cases is by adding a differential or transmission in the system between the upper and lower body connections.

The goal is to create a compliant transmission system which transfers the motion from one leg to the other when walking. Classical transmission systems are for instance gears and couplings, transferring motion and power from one part of the system to another. These systems often show wear over time due to friction and hysteresis between the different components, besides that they are heavy and often labor intensive to assemble. A relatively new field of research on compliant mechanisms provide solutions to these problems. Compliant mechanisms offer great opportunities as they contain a very limited amount of parts, reducing the weight of the structure and the manufacturing cost as almost no assembly is required. Besides that, the mechanism can easily be scales for different sizes or applications. Examples of concepts for compliant transmission systems can for instance be found in [[6],[9], [2]].The literature review in section 2 gives a more in depth overview of concepts and research on compliant transmission systems.

For the transmission system to be applicable in the Laevo, it should be shaped as an hip brace which is on both ends connected to one of the legs. The mid of the transmission will be connected to the upper body. To obtain the desired transmission behaviour, a low torsion stiffness should be obtained in this beam like structure. To maintain the bending support properties, the decrease of the torsion stiffness can not influence the bending stiffness off the system too much. Some research has been done in tuning and reducing the torsion stiffness in structures, mostly in applications for wings [[1], [4], [8]]. All

of these concepts are based on straight structures. The technical paper in Section 3 goes into detail how some of the design principles of previous research can be applied in the design of the desired transmission system. After the technical paper, Section 4 will go into how the design can be tuned to meet the requirements from the Laevo exoskeleton use case.

Besides the three chapters, additional information on this project is provided in this report, gathered in the Appendices. Appendix A, containing additional information on the technical paper, such as the manufacturing method, the measurement setup and measurement data. After which follows Appendix B, containing additional information on the concept generation and the initial prototyping process.

2

Literature review

Literature review on transmission systems in compliant mechanisms

R.F.L. Gerlach, 5173907
Thesis MSc. Mechnical Engineering
PME department, Technical University of Delft

***Abstract*—Compliant mechanisms can offer great benefits in replacing traditional mechanisms in terms of wear, friction, and manufacturing. An example of these classical mechanisms are transmission systems, for which compliant designs are currently in development, and to some extend, already applied. One of the main challenges in the application of compliant mechanisms lies in the loss of strain energy due to the deformation of the flexible members. To bring real improvement compared to the traditional transmission systems, this feature needs to be improved to enhance the energy efficiency. Different methods can be applied to obtain this result such as: size optimization, parts reduction, and (static) balancing of the system. This paper gives an overview of current designs for compliant transmission systems, shows the energy efficiency characteristics of these mechanisms, and identifies methods to enhance the efficiency for future designs.**

***Index Terms*—Compliant Mechanisms, Transmission, Energy efficiency**

I. Introduction

Compliant mechanisms are a relatively new field of interest within engineering. The behavior and working principle of compliant mechanisms is based on the deflection of flexible members. In traditional engineering, the main focus is on rigid structures connected by joints and hinges. When looking at nature we see much more flexible and compliant structures performing high precision tasks at high speeds. This is one of the main inspirations for compliant mechanisms. Compliant mechanisms are usually more complex to design as different functions are combined into fewer parts. However, it also offers many potential benefits. Possibilities in monolithic design reduce assembly and manufacturing efforts which can reduce the cost and enhance the performance of the product. Compliant mechanisms show relatively low amounts of wear and backlash and increase the precision of the mechanism. Other advantages include; no need for lubrication, low weight, and scalability [1].

These benefits can be observed when using the principle of compliant mechanisms in different applications. Compliant transmission systems can offer great benefits when used in combination with traditional mechanisms. Therefore an increasing number of mechanisms are designed in a compliant manner, which has led to a demand for integrated compliant transmission systems increases. Traditional examples of transmission mechanisms are couplings, gears, and linkages. They all provide a controlled manner of transferring input motion and force of a source. Couplings usually provide a conversion of the direction of motion of the input source, which is usually rotating. Gears convert torque and speed from the input- to the output port [2]. Most of these systems hold many separate parts between which friction and hysteresis arise, leading to damage and energy losses. Making the systems compliant could prevent these disadvantages. Besides that, it will create opportunities to make transmission systems on a much smaller scale.

The scalability and possibilities concerning fabrication create great opportunities for the application of compliant transmission systems on the micrometer scale, and possibly even smaller. An example, where this is already broadly applied, is in Micro Electronic Mechanical Systems (MEMS) applications. Before this literature review, Iqbal and Malik [3] have already reviewed amplification systems in MEMS applications. The biggest category within this review is compliant mechanisms. Some of the mechanisms used in the review will also be mentioned in this paper. Besides MEMS, robotics is a field where compliant transmission systems are often used. Hricko made an overview of compliant mechanisms for motion and force amplifiers for Robotics [4]. Many of these mechanisms are similar to examples mentioned by Iqbal and Malik, underlining the ease of scalability and wide possibility for application of the designs. A more specific review is done by Lewis et al. in [5], focusing solely on compliant transmission mechanisms for bio-inspired flapping-wing micro air vehicles. In this application, the reduced weight of the compliant mechanisms results in great benefits. Most of the examples mentioned up until now focus more on the compliant transmission variants of gears rather than couplings. Machekposhti et al. presented a review on compliant joints and rigid-body constant velocity universal joints in [6] which emphasizes the possibilities for compliant couplings.

The aim of this paper is (i) To create an overview of current research and applications for compliant transmission systems (ii), To investigate the energy efficiency of these systems, and (iii) To determine how the energy efficiency is optimized or could still be improved. As mechanisms that are characterized by the general function of transmission systems are not always referred to as such, the search for compliant mechanisms will be guided by the definition of a transmission system. The main definition mentioned in the Dictionary of Mechanical Engineering [7] states that a transmission should be a system that transmits power and torque from a power source. As this definition is broad, a second definition will be used as stated in [8] which describes it is as an element that matches the integrated actuator-transmission system to the load characteristics of the application.

One of the current downsides across all applications when using compliant mechanisms, generally, is the strain energy arising in the flexible members. This, often undesired, storage of energy, can lead to high stresses and loss of energy efficiency (mechanical efficiency) of the system [8]. As the main aim of a transmission is to transfer power, the efficiency of the mechanism is an important parameter to measure the performance.

To obtain the literature for this review multiple scientific search engines and search terms are used. Important search terms and synonyms that are used include: (i) Compliant, elastic or flexible, (ii) Mechanism, system or structure, (iii) Design, modeling or analysis, and (iv) Transmission, amplification, coupling or clutch.

In the following section, an introduction is given on the topic of energy efficiency in general and energy efficiency in compliant mechanisms. This section is followed by the Method II, explaining the method used to obtain the literature and how the literature is categorized. The literature will be presented in the Results III chapter. At the end of this section, an overview is shown of the characteristics of the presented mechanisms. The last part of this paper includes the Discussion section IV, which will go into the comparison between the different systems and potential trends, and in the end, the Conclusion V, summarizing the results obtained in this review.

A. Elaboration on energy efficiency

The efficiency of most mechanical structures is usually determined by comparing the ratio between the in- and output power. This approach is an effective manner of comparing different mechanisms, as the power of different types of mechanisms either mechanical or electrical, can easily be determined. For transmission systems, the in- and output power are determined in terms of force and displacement which result in the mechanical efficiency η as can be seen in Equation 1[8].

$$\eta = \frac{P_{out}}{P_{in}} = \frac{\int F_{out}(t)u_{out}(t)dt}{\int F_{in}(t)u_{in}(t)dt} \tag{1}$$

The efficiency of conventional mechanisms can be influenced on material level such as stress and strain as well as external factors such as friction, backlash, and fabrication errors. Compliant mechanisms are known for eliminating many of the external factors but show a decrease in efficiency on material level.

The working principle of compliant mechanisms is based on the deformation of flexible members, this inherently means that strain energy is present in the mechanism. The strain energy present in the material is a result of the input energy transformed into the desired deformation. When the input energy is decreased, the deformed mechanism often goes back to the original state, and the strain energy stored in the material is lost [9]. Optimizing structures, in terms of energy efficiency, usually leads to volume reduction as this means less strain energy necessary for deformation. Up until a couple of years ago, the assumption was made that this strain energy always needed to be added to the system. This resulted in the conclusion that a compliant mechanism would probably never have an efficiency higher than 80 %. [8].

There are various methods to synthesize and optimize structures for this purpose. Zhu et al. describe multiple objective functions concerning the energy usage of the system for topology optimization in [10]. When using mechanical efficiency as the main objective for optimization, the strain energy, stored in the system, will be minimized. This efficiency objective can be used for size and shape refinement as well ass topology synthesis. Nevertheless, performing topology optimization for a design increases efficiency, but often the losses due to strain energy will still occur.

Recently researchers have been experimenting with mechanisms that have the strain energy for deformation stored into the mechanism. This decreases the amount of energy needed as input for the system to obtain the same output, resulting in more efficient systems. The work done on energy-free systems by Herder [11] is an example of research on and concepts of statically balanced mechanisms. The statically balanced systems are characterized by the continuous equilibrium present in the mechanism. The equilibrium of a system can be determined by looking at the potential energy present. Creating continuous equilibrium results in constant potential energy. The application of this concept of constant potential energy is used in compliant mechanisms, for instance by Rijff and Herder [12] and Radaelli, Gallego, and Herder [13].

II. METHOD

To create a clear overview of the current state of research and applications in compliant transmission systems we present a classification in Figure 1. The classification is done along two axes, one concerning the compliant characteristics of the mechanism and the other one the transmission system characteristics. From research, we can determine a trend in the design approach which is often determined by the application of the compliant mechanism.

The scale of the design will be used along the compliant mechanism axis. The size of the mechanisms is a continuous variable that can be plotted as the area of the mechanism in x- and y-direction. The two axis describing the largest area are used for each mechanism, leaving out the third dimension, which is usually the thickness. To make a discrete categorization, the size of the mechanism is transferred to three scale categories: micrometer, millimeter, and meter scale. The scale and motion categorization is shown in 2. It should be noted that usually the size of the prototype is used for

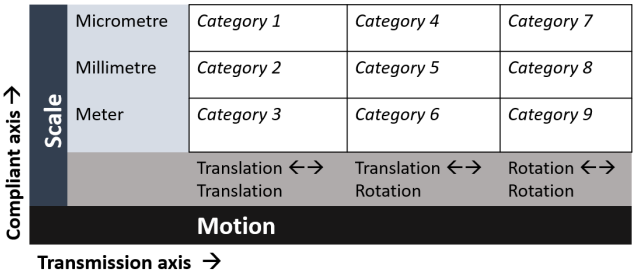

Fig. 1. Categories used for creating a literature overview

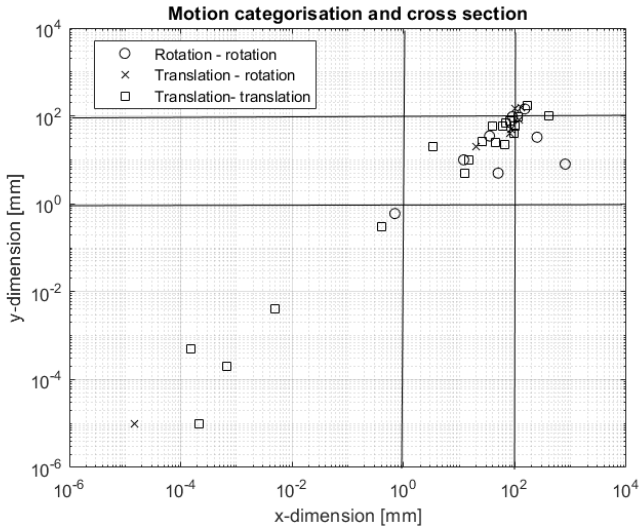

Fig. 2. X and y dimensions of the selected mechanisms combined with the categorisation for motion

this definition which can differ from the scale of the end application or possible applications.

For the transmission system characteristics, it is chosen to make a differentiation by means of the kinematics of the system. To determine different categories, the in- and output motion of the system is analyzed and defined in three groups. The three groups, shown in Figure 3; (i) Input translation towards output translation, (ii) Input translation towards output rotation (or the other way around) and (iii) Input rotation towards output rotation. Integrating the two axis into a scheme results in nine different categories.

The collection of relevant data was done by using multiple different search engines such as Research gate, Scopus, and Science direct. Relevant keywords and search terms used for the search are shown in Table I. To ensure all found mechanisms can be indeed classified as a transmission, they will be tested against the definition as given in the introduction. The most important question is: is its main purpose to transfer power or motion?

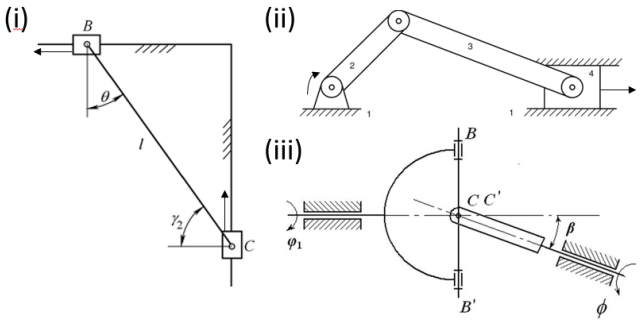

Fig. 3. Schematic presentation of the three motion types in classical transmission systems (i) Double slider, Translation- Translation [14], (ii) Crank- slider, Translation - Rotation [15] and (iii) Universal joint, Rotation - Rotation [16]

TABLE I
SEARCH TERMS

Keywords	Synonyms or similar
Compliant	Elastic, Flexible
Mechanism	System, Structure
Design	Modelling, analysis
Amplification	Geometrical advantage, mechanical advantage
MEMS	Micro systems, robotics
Transmission	Force amplifier, displacement amplifier, coupling, clutch

Besides a categorization, all mechanisms will be evaluated on their energy efficiency. Not for all mechanisms, energy efficiency is stated in the literature. Therefore, some other parameters will be used, which are usually concerned with energy efficiency: amplification, system stiffness and peak stress. When the in-and output displacement and force are given, the efficiency can be calculated using Equation 1.

III. RESULTS

The result of this literature review are presented for each of the nine categories defined in the previous section. When found, multiple examples of mechanisms are explained, as well as their performance in terms of energy efficiency. In the end an overview of these performances will be given.

A. Translation- Translation

When a transmission system had a force with a translational motion as input and a force with a translational motion as output, it is characterized to be Translation - Translation. The type of motion does not specify the plane or space used by the mechanism. Within this category, a distinction is made between different sizes of mechanisms. Applications often seen in this section are motion or force amplification systems. To create a clear picture of each of the size and motion combinations, one example will be elaborated on for each category.

1: Micrometre scale mechanisms

Smart material and electrothermal actuators are often used

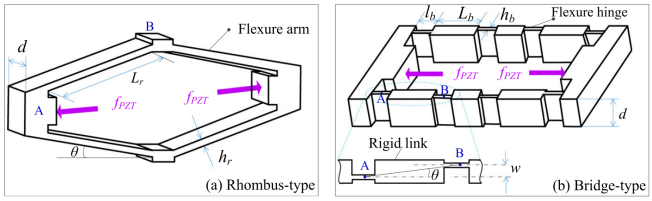

Fig. 4. Displacement amplification transmissions for piezoelectric compliant mechanisms a)Rhombus-type and b) Bridge-type [19]

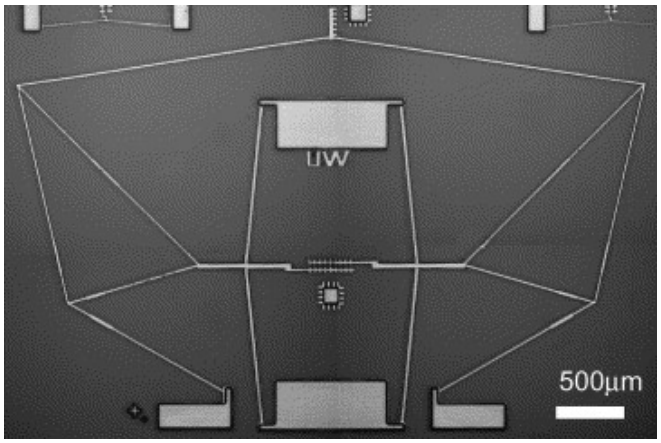

Fig. 5. Compliant micro transmission for rectilinear electrothermal actuators [21]

in microscale applications such as MEMS, due to their high output force and low actuation voltages. However, most of these actuators have a very limited output stroke. Because for many applications a larger output stroke is required, a transmission system will be used to amplify the actuator stroke. These systems are also often referred to as displacement amplification systems. Research and design of this kind of system is done by many. Some of the most used systems are the Scott-Russel mechanism, as described by Tian et al. [17] and Ha et al. [18], the Rhombus-type and Bridge-type mechanism as described by Ling et al. in [19] are often used. The Rhombus- and Bridge type can deliver a displacement amplification up to 15 and 25 times the input displacement respectively.

Some of these mechanisms are even developed further and used as the base for more complex systems. This is done by Ling et al. [20] by using the Rhombus concept to create a multistage displacement amplification mechanism. A less known design for motion amplification is the compliant micro transmission for rectilinear electrothermal actuators as developed by Chu, Hetrich and Gianchandani [21] which is shown in Figure 5. The thickness of this mechanism is 11.5 μm and is made out of Silicon and Nickel. It amplifies the input displacement twenty times. Due to design constraints concerning the minimum width of the mechanism, more energy than necessary is lost in the deformation of the flexible

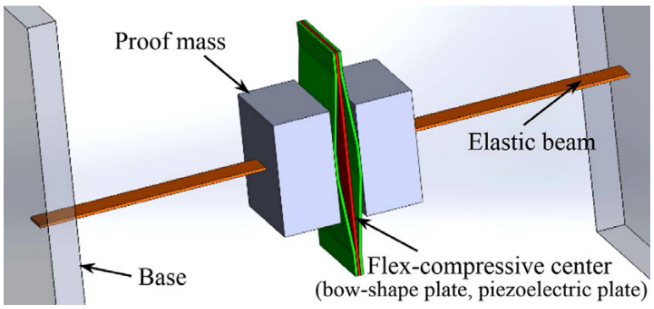

Fig. 6. High-efficiency compressive-mode piezoelectric energy harvester (HC-PEH) [27]

members of the mechanism, this results in an efficiency of only 14.1%.

2: Millimetre scale mechanisms

Within this category an overview of mechanisms for which we can find the application in micrometer systems, precision stage systems, and robotics is given. Often, the first prototypes of displacement amplification mechanisms are developed at this size to later be scaled down for MEMS applications. Examples of this can be found in research done by Lai and Zhu in a bridge-lever displacement amplification mechanism [22], Sun and Yang with a flexure-hinged displacement amplification system [23] and the five-bar compliant mechanical amplifier developed by Ouyang, Zhang & Gupta [24].

Nevertheless, there are also mechanisms applied at this scale. The applications of these mechanisms show great variation from micro frequency quadrupler transmission systems as developed by MacHekposhti et al. [25] to compliant microgrippers, as developed by Kumar et al. [26], but also high-efficiency energy harvesters, as developed by Yang and Zu [27]. This compliant energy harvaster is able to obtain energy from ambient vibration energy. The vibrations result in the bending of elastic beams attached to the base, this creates an compressive force on the proof mass which results in tension on the Flex-compressive center. An overview of the mechanism is shown in Figure 6. To facilitate the characteristics of piezoceramics, small strain and large ultimate stress, the mechanism contains a multi-stage force amplification system. The resulting design can yields up to 1000 times more energy, using the same circumstances compared to conventional flextensional energy harvasters. Compared to other relatively new energy harvasters, it still produces upto 10 times more energy. However the dimensions of the current design are not optimized yet and could be improved even further.

Another example is a friction-based locking device actuated by PZT-stack actuators as developed by Tschiersky and Berselli et al. [28]. As the output displacement of the PZT-stack actuators is limited, a displacement amplification

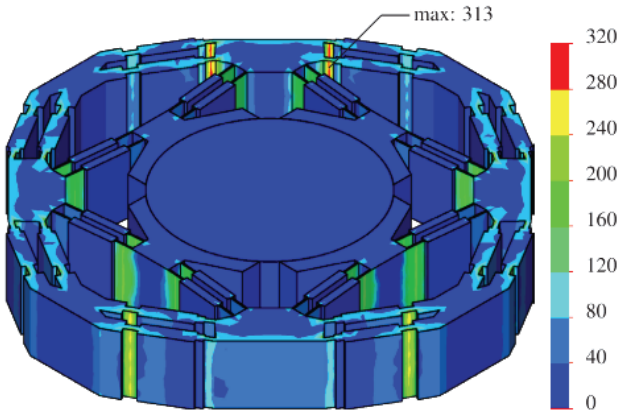

Fig. 7. Stress distribution in MPa for PZT-actuated compliant locking device [28]

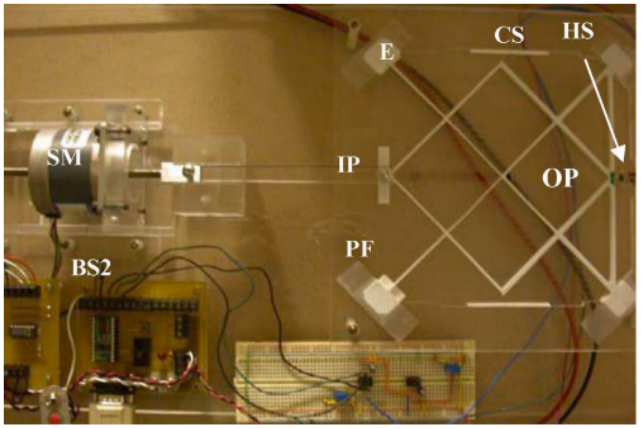

Fig. 8. Compliant Transmission Mechanism With Intermittent Contacts for Cycle-Doubling [31]

is required to go from unlocked to the locked state of the device. However the force is also a very important performance parameter for a locking device, therefore this is also taken into consideration in the optimization of the mechanism. Optimizing for displacement and force directly means optimizing the mechanical efficiency of the system as the in- and output power are determined by the displacement times the force.

Figure 7 shows a stress plot for the locking device made from a SolidWorks simulation. The mechanism has a diameter of 69.96 mm and a thickness of 10 mm. The force transmission ratio varies from -14.1 with no contact, up to -18.7 when in contact with a rotating axis. In this mechanism, a lot of energy is lost in the deflection of the flexible members transferring the power from the input towards the output. The final design can apply a holding torque of 1.9 Nm.

3: Meter scale mechanisms

For the meter scale translation mechanism, the working principle is often not based on the distributed deflection of beams, but based on lumped deflection. This can be seen in examples such as the pantograph, developed by Ishii, Thümmel & Horie [29], and the tensural displacement amplifier employing elliptic-arc flexure hinges developed by [30]. This is possibly because the exact kinematics become harder to determine for longer flexible elements.

However not all systems use this principle. Mankame and Ananthasuresh present a transmission mechanism that can double a cyclic input frequency in [31]. A macro-scale prototype was build which is shown in Figure 8. Nevertheless the mechanism should be easy to scale due to the monolythic design, which can be manufactured out of many different materials for a large range of length scales. Dynamical analysis are also done for macro and meso scale. The efficiency of the mechanism ranges from 14.2% up to 21.5 % depending on the loadcase. The main factor mentioned to have

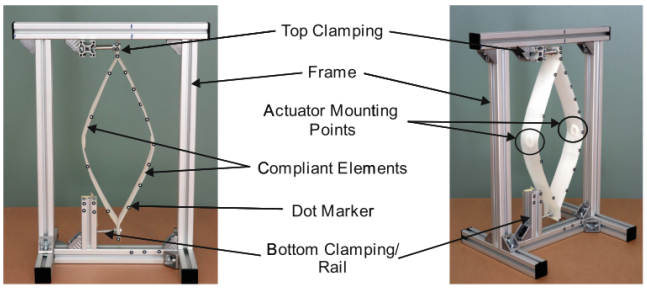

Fig. 9. Deltoid mechanism demonstrator [32]

a significant contribution to this relatively low efficiency is the input energy needed to deform the mechanism. Proposed solutions include: smaller deflections for the flexible bodies and preloading. Friction does not seem to have a significant contribution to the efficiency in this design.

Another example is the deltoid mechanism used for motion transmission in civil engineering machinery by Steinbild and Zhang et al. [32] which uses distributed deflection of two flexures to transfer an upward input towards a sideways output. The aim of the transmission is to protect the actuator by decoupling or damping forces from the environment. One of the possible applications could be in vibrating tampers. The demonstrator of the mechanism can be seen in Figure 9.

To enhance the efficiency of the mechanism, the supply of electric current is timed to be in phase with the oscillation. This results in less energy consumption for a larger displacement. The maximum displacement is an input of 13.1 mm which results in an output of 11 mm. The structure is not balanced as reaction forces are present in the attachment point on the upper side of the system.

B. Translation- Rotation

This section describes transmission systems that transfer the motion from translation to rotation. Systems often seen in this

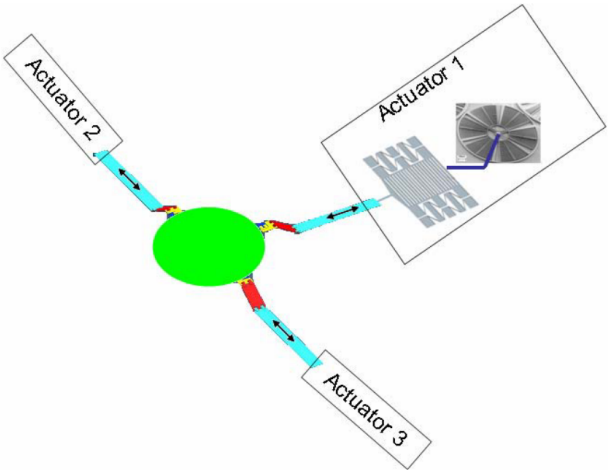

Fig. 10. Schematic of compliant rotary-to-translational transmission mechanism for a micro-parallel kinematic mechanism (not to scale) [33]

section are compliant variations of crank-slider mechanisms.

4: Micrometre scale mechanisms

Not many examples are yet developed at the micrometer scale for systems transferring translational motion to a rotation. Only one example is found, however, no prototypes on this scale are made. The compliant rotary-to-translational transmission mechanism developed by Bronsen, Wiens and Fassi [33] is based on a slider-crank transmission system. The slider-crank mechanism is made compliant by using a Robert's mechanism, as can be seen in Figure 10. The system is designed for micro/nanopositioning and manipulation of optical components such as mirrors and lenses. From the analytical model, the relationship between the voltage and output displacement can be obtained. Efficiency or energy usage are not determined.

5: Millimetre scale mechanisms

Planar examples often include compliant designs for traditional crank-slider mechanisms or cam-follower mechanisms. An example in which both principles are applied is developed by Giraud, Zhakypov and Paik [34]. The design is made out of different layers of composite material, creating a quasi-2D stack. It can convert rotation to translation, in and out of plane. The system is shown in Figure 11 the stack mechanisms are shown for the slider-crank and the cam-follower mechanism. The maximum displacement of the cam-follower and slider-crank mechanism are 3 mm and 7 mm with an input force of 0.35 N and 76 N respectively. Optimization for these designs still needs to be done for the friction losses in the pin joints and the material and geometry of the flexible components. Another example of a slider-crank mechanism is developed by Pardeshi, Kandharkar & Deshmukh [35]. Besides these, mostly planar examples, a spatial example should be mentioned developed by Ortha and Yilmaz [36]. This design exists out of multiple discs

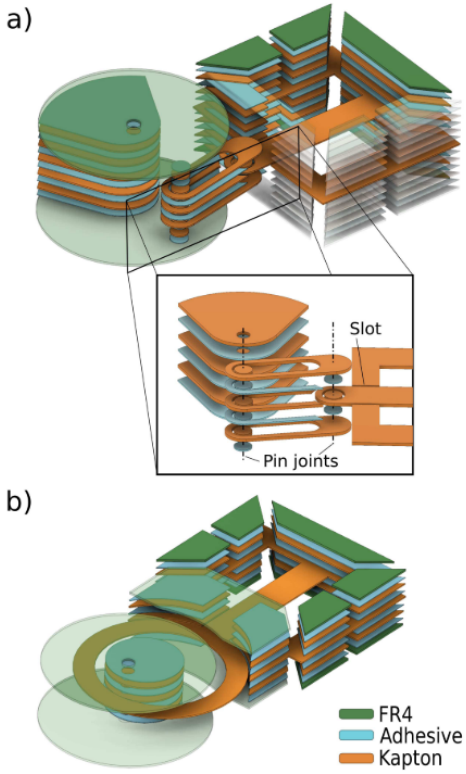

Fig. 11. Low-Profile Compliant Transmission Mechanisms a) Slider-crank b) cam-follower [34]

connected by flexures which deflect when the top disc is loaded by a moment, resulting in a motion downwards towards the fixated disc.

6: Meter scale mechanisms

Translation to rotational movement is also used in motion stages such as the compact flexure-based precision pure rotation stage by Clark et al. [37]. The mechanism is 128mm x 153mm x 30mm and has a working range of 2.540 mrad. It exists out of two layers as shown in Figure 12. The mechanism is optimized for precision in the end effector. As neither high forces nor large displacements are desired, the energy efficiency is not used as an performance indicator in this mechanism.

C. Rotation - rotation

To convert a rotating motion from one axis to another, couplings and clutches are often used. These serve the purpose of aligning the axis of the input moment and the output load. An a broader perspective, another example can be a revolute joint. A universal joint also allows for alignment of two rotating axis, even if they are slightly tilted. In general we see more mechanisms performing this motion transfer for larger applications, as rotational actuators are more commonly used.

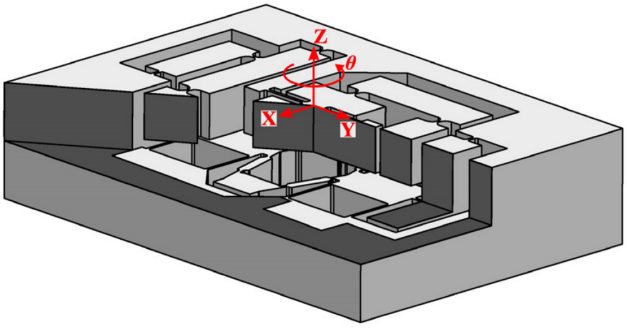

Fig. 12. Compact flexure-based precision pure rotation stage without actuator redundancy [37]

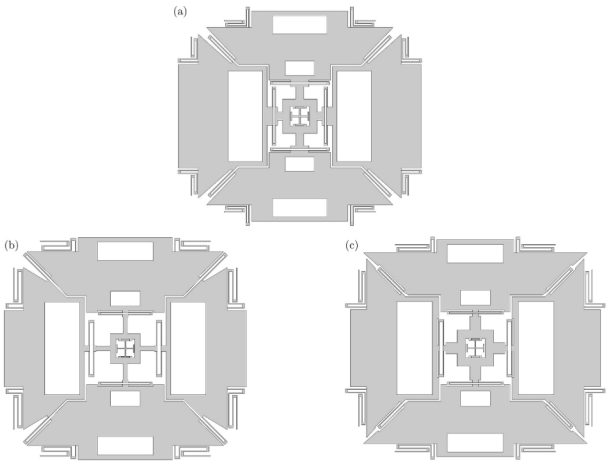

Fig. 13. Triaxial beating-heart MEMS gyroscope a) initial guess b) optimized for sensor response c) optimized for spurious modes frequencies [38]

7: Micrometre scale mechanisms

Very few systems are known for transferring rotational motion into another rotating axis for micro-scale mechanisms. This can be explained due to the manufacturing limitations for micro-scale mechanisms, which mostly support planar mechanisms. Besides that most actuators on micro-scale are linear and therefore there is no real demand for transmission systems converting rotational actuator input. However, some sensors do use this principle.

An example of an application is the triaxial beating-heart MEMS gyroscope, developed by Gianni, Bonaccorsi & Braghin [38]. In the gyroscope, one of the objectives in the optimization process is to maximize the displacement to maximize the sensor response. When comparing the optimized structure in Figure 13 b) with the initial structure in a), we can see that the system has less material and more slender beams. This will result in less energy which will be lost in the deformation process of the system, creating a more energy efficient mechanism.

8: Millimetre scale mechanisms

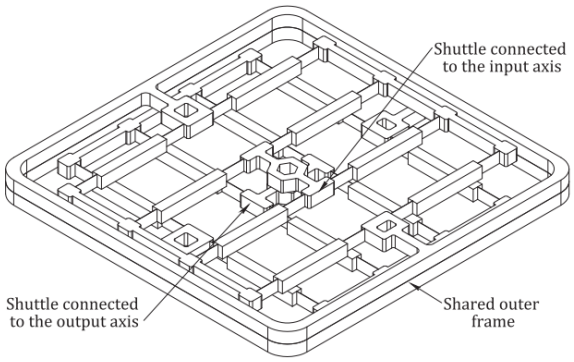

Fig. 14. Statically balanced fully compliant power transmission mechanism between parallel rotational axes [39]

An important application for rotation to rotation transmission systems is the alignment of rotating axis. Limited research has been done into this aspect for compliant mechanisms. Machekposhti, Tolou and Herder developed such a concept [39], as depicted in Figure 14. The statically balanced fully compliant power transmission mechanism is based on the principle of an Oldham Coupling. The mechanism prototype is 50 mm x 50 mm x 0.2 mm. The experimentally obtained actuation torque is in the order of 10^{-5}Nm and can therefore be assumed to be zero. The efficiency of the system is significantly increased by static balancing of the internal stiffness, resulting in zero actuation stiffness. Besides that it has less friction, backlash and assembly errors compared to the classical coupling.

If we look at this in a broader perspective and search for the working principle, we can find universal- or revolute joints as can be seen in [6] and designs developed by Tanik et al. such as [40] and [41] for fulfilling a similar alignment purpose. It is also often used due to the constant-velocity characteristics of the mechanism.

An other example is shown in Figure 15, a spherical four-bar mechanism [42]. The mechanism is optimized for maximum output rotation while constraining the deflection in the flexible members. The resulting mechanism can achieve relatively large rotations without plastic deformation.

9: Meter scale mechanisms

For larger applications, the transfer of rotational to rotational motion becomes more important as rotational actuators are more common. One application of these actuators can be found in the control of joints in active exoskeletons. A transmission system is often preferred as input motion frequency and desired output frequency do not match. Another problem is the placement of the actuators. For the weight and efficiency of the system, it is beneficial to have the placement not always near the joints. To then transfer the motion from the actuator to joints, a compliant transmission systems such

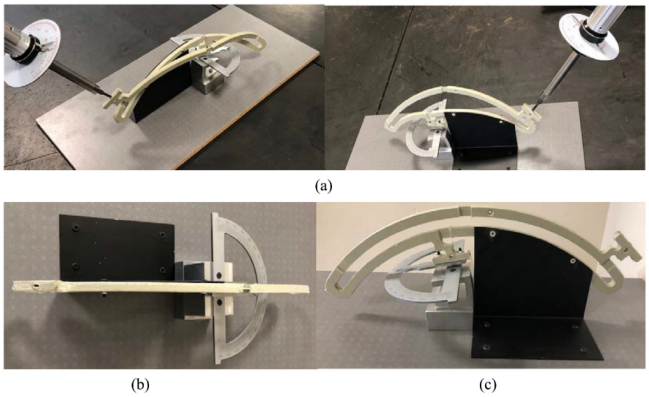

Fig. 15. Three different views on the prototype testing of a spherical four-bar mechanism a) test- set-up, b) top view and c) front view [42]

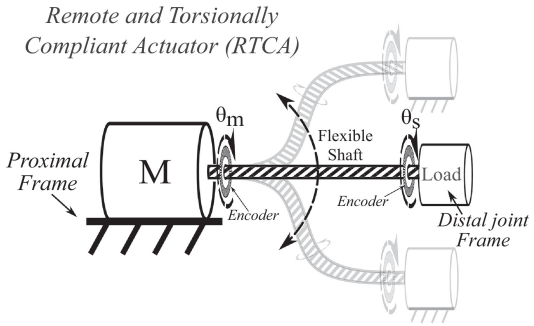

Fig. 16. Remote Torsionally Compliant Actuator (RTCA), System in bending radii [43]

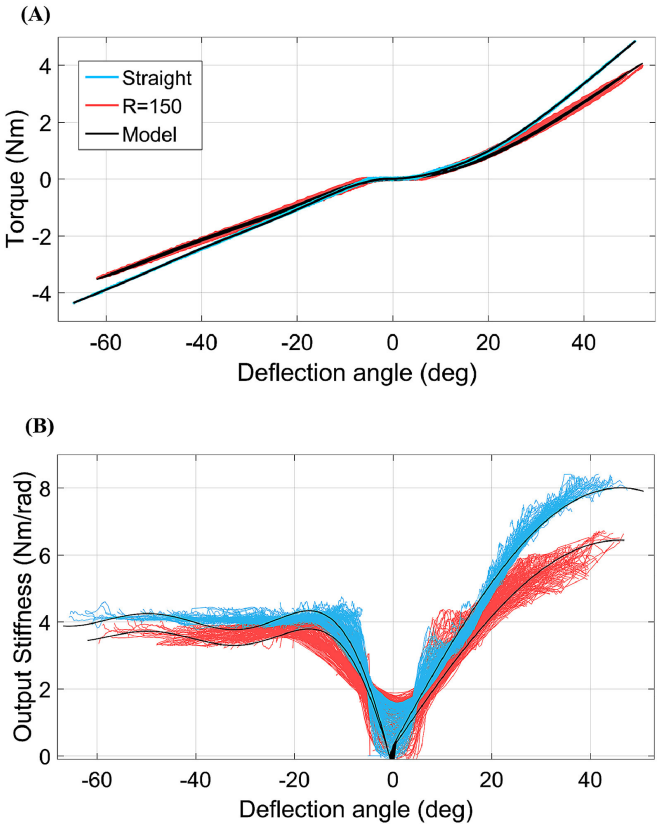

Fig. 17. Remote Torsionally Compliant Actuator (RTCA) a) Torque for different deflection angles and bending radii, and b) Stiffness for different deflection angles, straight (blue) and R=150 mm (red) [43]

as included in the Remote Torsionally Compliant Actuator (RTCA), developed by Rodriguez-Cianca et al. [43] can be used. The system is shown in Figure 16. The energy efficiency of this system is dependent on the deflection angle resulting from the position of the actuator relative to the load. The best results are obtained in an aligned configuration. The highest losses occur when the flexible shaft has a bending radius of 250 mm and are respectively 18% and 29% in comparison to straight conditions. The results suggest that for this bending angle friction occurs between the internal layers this results in higher energy loss and a lower stiffness, as can be seen in Figure 17 a) and b). Note that the stiffness here is characterised in longitudinal direction and not in bending.

Another application in robotics can be observed in flapping-wing aerial vehicles. Zhang et al. [44] developed a compliant transmission to transfer the motion from the rotational actuator towards the wings. This mechanism is shown in Figure 18. Integrating the compliant transmission system can reduce the minimum torque by 73.9%, and the peak input torque of the system up to 66 % compared to the original non-compliant rigid-body mechanism.

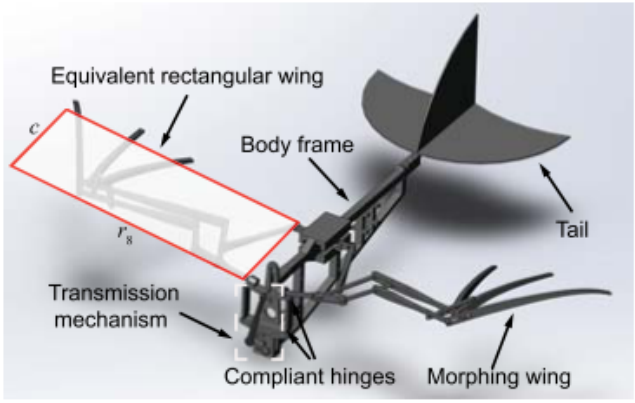

Fig. 18. Compliant Transmission Mechanism for Flapping-wing Aerial Vehicles [44]

D. Overview

Table II gives an overview of the efficiency of the compliant transmission systems found in literature. Besides the energy efficiency, other performance indicators are discussed such as amplification, peak stress, force/ displacement, design space and the material. These parameters are determined either by experiments with a prototype or numerical modelling. The amplification is determined by the output displacement divided by the input displacement, this indicator can be linked to efficiency as more efficient systems are able to create relatively larger output displacements. The $*$ indicates that the amplification is not always the same and a maximum value is presented. However it is not the same as the force is not taken into consideration [8]. The force divided by the displacement is also known as the stiffness of the system, as force as well as displacement are taken into consideration in this indicator, it gives a good estimation of the efficiency of the system.

Not all information on these indicators is available in literature, therefore an overall judgement on the efficiency is given in three different levels: low ([L], 0-40%), middle ([M], 40-70%) and high ([H], 70-100%). This judgement is based on a combination of the performance indicators shown in the table and descriptions of the authors of the papers on short comings and performance compared to other alternatives. If there is no indication given about the efficiency of the systems, it will be marked as 'N/A'. When the efficiency is available in literature, the exact number or range is given. When the efficiency is estimated the ranges, as described before, for each efficiency category are given. Both these given and estimated efficiencies are accompanied with the category by means of a letter L, M or H for Low, Middle and High. The mechanisms for which the efficiency is given or estimated, are investigated in more detail, which are presented in Figure 19.

For most of the mechanisms an optimization method is used to enhance the performance of the system. However, as the requirements and constraints of each system differ, the objective of the optimization also varies. In Figure i) 19 the main objective for the optimization of the mechanism is shown for each of the mechanism in the different efficiency categories. It is clear that for all the mechanisms that optimize their structure for mechanical efficiency, the highest efficiency is obtained. Only three mechanisms discussed in this paper are explicitly optimized on efficiency. These include: The torsionally compliant actuator [43], the double slider mechanism [45], and the power transmission between rotating axis [39]. The 'Others' group contains objectives concerning the frequency of the mechanism or coupling characteristics such as transformation of motion or alignment.

For each of the mechanisms a number of different methods are used to create the optimal design. Figure ii) 19 shows these

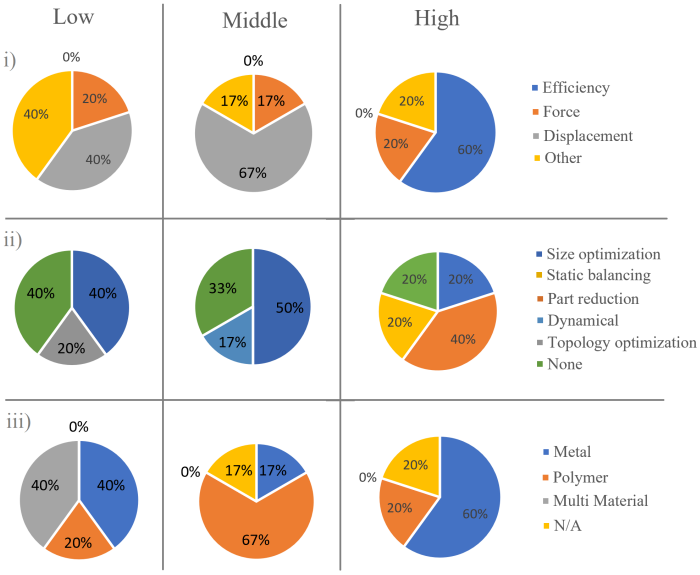

Fig. 19. The three different categories of energy efficiencies, low middle and high combined with the: i) The objective of the optimization method applied, ii) The method applied in the design process for optimizing the mechanism and iii) The material used.

methods distributed over the different efficiency categories. When analysing these results, the results from the previous graph should be taken into consideration; not for all methods applied the aim is to optimize the efficiency. Nevertheless, the high efficiency mechanisms is the only category which applies the static balancing method, such is done in the power transmission between rotating axis [39], which is optimized on the efficiency. Besides that it can be obtained from this figure that topology optimization did not lead to high efficiency systems. Topology optimization is applied in the Cycle-doubler mechanism in [31], which is optimized for the frequency and not necessarily for efficiency.

Size optimization is often done by using optimization algorithms based on analytical models. Examples of mechanisms where this method is applied include the cycle doubler by [31]. However many factors are not taken into consideration in the optimization process, such as friction, large displacements, and manufacturing-induced features. The paper on the compliant transmission for secondary microactuators in disk drives presents an optimization method that maximizes the energy efficiency of the transmission while constraining other parameters as maximum stress, natural frequency, and axial loading. Optimizing energy efficiency often leads to volume reduction as this means less strain energy in the mechanism. An example can be seen in Figure 13, the MEMS gyroscope developed by Giannini et al. [38]. The structure optimized for minimum optimized for the sensor response shown in b) has a more slender structure compared to the other designs.

Neutral stability in a mechanism is obtained by aiming for constant potential energy. This means no strain energy needs to be added to the system to facilitate the deformation. This results in a mechanism where a very minimal amount of energy needs to be added to obtain the desired motion. The constant potential energy is usually obtained by trapping energy in the system for instance by applying pre-stress or adding additional springs to the system. An example of the application of this method is the statically balanced fully compliant power transmission mechanism from Machekposhti, Tolou, and Herder as presented in Figure 14. In the micro frequency quadrupler developed by Machekposhti et al. [25] it is also proposed to further develop the mechanism by adding preloaded beams to obtain static balancing and reduce the actuator force.

Parts reduction is generally already one of the features of compliant mechanisms which enhances the efficiency compared to non-compliant mechanisms: multiple functions are merged into fewer components. Fewer parts in the mechanism result in fewer parts in which energy is lost. To further increase the efficiency of these compliant mechanisms it could be investigated to further merge the functionality of the components, this was applied in the Torsionally Compliant Actuator (RTCA) by Rodriguez-Cianca et al.[43] Traditionally Bowden-cables are used to fit a similar purpose. However, in these systems forces are transmitted and not torques, this leads to the need for an additional mechanism which transfers the force into torque, making it less efficient.

Dynamically, the energy efficiency can be enhanced by matching the input signal to the oscillations of the mechanism as is done in the deltoid mechanism presented by Steinbild et al. in [32]. This method could be applied by using the eigenmodes of the structure to increase the energy efficiency. This is for instance applied in compliant robotics such as the walking insect of Schonebaum [46].

Topology optimization or continuum topology optimization is a new method in optimizing the structure for compliant mechanisms. Instead of only optimizing the length and thickness of different parts, it also optimizes the shape and topology of the system. It uses an initial structure or volume with loading conditions as the input. The optimization structure then composes a design that is most suitable for the desired objective. A review of applying this method on compliant mechanisms is done by Zhu et al. in [10]. Most of the objective formulations described in the literature in this review are even directly related to the energy (mutual strain energy, strain energy, input work, and mechanical efficiency) or a derivative of the energy (Geometrical advantage and Mechanical advantage). Continuum topology optimization was used in the optimization of compliant force amplifier mechanisms for surface micromachined resonant accelerometers by Pedersen and Seshia in [47].

In Figure iii) 19, for each efficiency category, the material of the mechanism is shown. The materials are split up in four different categories: Metal, Polymer, Multi-material and N/A. It is clear that within the found mechanisms, metal is often used in very efficient mechanisms, such as the energy harvester mechanism [27] or the power transmission system of [39] Besides that it can be obtained that multi material mechanisms such as the Low-Profile compliant transmission from [34] or the Micro transmission in [21] show very low efficiency. However it should be noted that the material mentioned in the literature often reflects the material for the prototype and not the final application.

TABLE II
RESULTING EFFICIENCY INDICATORS FOR ALL MECHANISMS

	Name	Efficiency	Amplification	Peak stress [Pa]	Motion	Stiffness [N/m]	Area [mm3]	Material	Efficiency method	Source
1	Deltoid Mechanism	52.69% [M]	5.78E-01	N/A	T-T	8.00E+03	6.93E+04	Polymer	Dynamical	[32]
2	Amplifier	N/A	2.86E+01	5.83E+08	T-T	N/A	4.00E+04	N/A	Size optimization	[48]
3	Cycle-doubler	21.50% [L]	2.00E+00	1.87E+01	T-T	N/A	2.89E+04	Polymer	Topology optimization	[31]
4	Rotation stage	N/A	2.80E+00	N/A	T-R	N/A	1.96E+04	Polymer	Size optimization	[37]
5	Variable stroke mechanism	N/A	variable	N/A	T-R	N/A	1.50E+04	Polymer	none	[49]
6	Tensural displacement	52% [M]	40*	1.36E+01	T-T	9.38E+00	1.07E+04	Polymer	none	[30]
8	Transmission Mechanism	70-100% [H]	1.00E+00	N/A	T-R	1.27E-01	8.20E+03	N/A	none	[44]
9	Torsionally Compliant Actuator	50-99% [H]	1.00E+00	N/A	R-R	N/A	6.40E+03	N/A	Part reduction	[43]
10	Pantograph	N/A	5*	N/A	R-R	N/A	6.00E+03	Polymer	none	[29]
11	Bridge-lever type	N/A	2.75E+01	5.09E+07	T-T	N/A	6.00E+03	Metal	Size optimization	[22]
12	Locking device	40% [L]	1.80E+01	3.13E+08	T-T	1.11E+07	4.89E+03	Metal	Size optimization	[28]
13	Slider crack mechanism	N/A	1.40E+00	3.37E+08	T-T	2.86E+04	4.20E+03	Metal	none	[35]
14	Energy harvester	70-100% [H]	1.02E+02	N/A	T-R	N/A	3.92E+03	Metal	none	[27]
15	Displacement amplifier	N/A	8.00E+00	1.16E+02	T-T	N/A	3.60E+03	Metal	Size optimization	[23]
16	Motion conversion mechanism	N/A	N/A	N/A	T-R	N/A	3.20E+03	Polymer	none	[36]
17	Amplification mechanism	0-40%[L]	1.21E+01	1.88E+08	T-T	1.24E+08	2.40E+03	Metal	Size optimization	[26]
18	Five-bar	40-70% [M]	2.43E+01	N/A	T-T	4.25E+06	1.43E+03	N/A	Size optimization	[24]
19	Scott-Russell	40-70% [M]	cot(theta)	N/A	T-T	1.93E+06	1.13E+03	Metal	none	[17]
20	Micro frequency quadrupler	N/A	1.20E-01	2.00E+08	T-T	2.00E+00	6.76E+02	Polymer	none	[25]
21	Low-Profile compliant transmission	0-40% [L]	N/A	N/A	T-R	2.00E+02	4.00E+02	Multi-material	none	[34]
22	Power transmission	70-100% [H]	1.00E+00	N/A	R-R	3.60E+02	2.50E+02	Metal	Static balancing	[39]
23	Multistage compliant	N/A	8.40E+00	5.00E+06	T-T	1.00E+08	1.50E+02	Metal	none	[20]
24	Compliant toggle linkage	N/A	1.00E+00	N/A	T-T	2.40E+02	6.80E+01	Polymer	Size optimization	[50]
25	Bridge-type	N/A	1.50E+01	1.60E+07	T-T	1.17E+05	6.25E+01	Metal	Size optimization	[19]
26	Rhombus-type	N/A	1.31E+01	1.90E+06	T-T	6.99E+05	6.25E+01	Metal	Size optimization	[19]
27	MEMS gyroscopes	N/A	1.00E+00	N/A	R-R	N/A	4.20E-01	Polymer	Size optimization	[38]
28	Accelerometer	40-70% [M]	N/A	N/A	T-T	N/A	1.20E-01	Polymer	Size optimization	[51]
29	Half scissor	40-70% [M]	1.30E+01	1.00E+08	T-T	2.54E+03	2.09E-03	Polymer	Size optimization	[52]
30	Microtransmissions	14.10% [L]	20*	N/A	T-T	6.13E+06	2.00E-05	Multi-material	none	[21]
32	Double slider mechanism	92.96% [H]	5.65E-01	N/A	T-T	1.08E+02	7.50E-07	Polymer	Size optimization	[45]
33	Single-stage microlever mechanism	N/A	20*		T-T	N/A	2.10E-09	N/A	Size optimization	[53]
34	Rotary-to-translational transmission	N/A	N/A	N/A	T-R	5.02E+01	1.50E-10	Polymer	none	[33]
35	Universal joint with linear stiffness	N/A	N/A	N/A	R-R	7.20E+01	1.23E+03	Metal	Size optimization	[54]
36	Spherical four-bar mechanism	N/A	N/A	3.41E+07	R-R	N/A	1.20E+02	Polymer	Size optimization	[42]
37	Steel Cardan universal joint	N/A	N/A	7.29E+08	R-R	N/A	2.16E+04	Metal	Size optimization	[41]
38	Cardan universal joint	N/A	N/A	N/A	R-R	N/A	8.64E+03	Polymer	Topology optimization	[40]
39	Compliant force amplifier mechanism	N/A	1.00E+02	N/A	R-R	3.50E-02	1.00E-07	N/A	Topology optimization	[47]

IV. Discussion

Table II gives an overview of the obtained efficiency characteristics of the mechanisms. For most of the mechanisms the efficiency analysis is not available in the literature, often only the kinematics is confirmed. Enhancing the efficiency would be possible future research. Besides that, the analysis of the dynamical behavior of the mechanisms is very limited. Performing this analysis could reveal potential pitfalls in energy efficiency as well.

In general, a trend could be seen in the type of systems most dominant in the different motion categories. The translation - translation category showed mostly force and displacement amplification systems. The translation - rotation category had many compliant designs of crank-slider mechanisms. The rotation - rotation category contained clutch and universal joint type of mechanisms. The last category tends to be more often optimized in terms of energy and achieves higher energy efficiencies. This can be seen in table II as 60% of the mechanisms found in the high-efficiency category are rotation - rotation mechanisms.

Two main conclusions can be drawn from the results shown in Figure i) 19. Firstly, not all mechanisms have the objective to be optimized in terms of energy efficiency. Often other objectives, such as force or displacement are used to enhance the systems. This is mostly the case when the other variable, stroke or force, of the actuator, are large compared to the desired output. Energy losses in the transmission system are then of less importance as the main goal can be achieved regardless. Displacement amplification systems are common in MEMS applications in combination with PZT-actuators. These actuators can produce a relatively high force but have a limited stroke, therefore the force is often not included in the objective of the transmission mechanism. The second, maybe obvious conclusion is that the systems of which the objective is to optimize efficiency, achieve the highest efficiency.

Besides the objective of optimization, also the method of optimization varies for the different mechanisms. Six design methods are identified to be applied in the optimization process of the different mechanisms. An overview of the methods in combination with the efficiency obtained can be seen in Figure ii)19. This figure shows that Topology optimization is currently only used in designs resulting in low efficiencies. This could mean that the method is not suitable for obtaining high-efficiency structures. However, as Topology optimization is a relatively new field of research, and a lot of development is happening, this method will probably still improve. Another remark may be made about the Static balancing method, which is only used in mechanisms leading to high efficiencies. Even though the number of examples in this paper is limited, Static balancing of compliant mechanisms shows great opportunities as it is the only enhancement method able to remove the strain energy, needed for deformation, from the input energy of the system. Lastly, size optimization is the most applied method of enhancement, probably as it could be done relatively easily and also results in lower cost.

Figure iii) 19 shows an overview of the materials mentioned in the literature concerned with the mechanisms. From this figure can be concluded that in high-performance systems, metals are often used. Metals have a wide range of manufacturing methods and the material properties can be modeled relatively accurately. Besides that, it can be concluded that multi-material designs often lead to lower efficiencies. This might be because the cooperation between different materials is more difficult to model and therefore more difficult to optimize.

Many of the current designs still indicate possible enhancements in terms of efficiency. The main sources of losses mentioned are; strain energy, electrostatic forces, and friction. Besides that, losses may occur due to viscoelastic behavior when using non-metal materials. The sources of energy loss can be divided up into two different categories; conservative forces, such as strain energy, and non-conservative forces, arising from friction and viscoelasticity. Static balancing offers a solution for countering conservative force, however, non-conservative forces can not be balanced or compensated for. Optimization techniques considering the shape or size of the volume may alter the conservative forces, but they can only be minimized. Friction can often be considered to be minimal in compliant mechanisms, nevertheless, besides friction, other non-conservative forces can be encountered in these systems.

As undesired energy losses still result in lower efficiencies for many transmission systems, it would be interesting to further investigate the application of the found solutions in a broader range of mechanisms. Besides that the development of new solutions will be an important research field in the progression of compliant mechanisms.

V. Conclusion

The purpose of this paper is (i) To create an overview of current research and applications for compliant transmission systems (ii), To investigate the energy efficiency of these systems, and (iii) To determine how the energy efficiency is optimized or could still be improved.

The overview is made using a classification scheme that holds nine categories, made up out of two axes: the motion of the system in terms of in- and output translation or rotation and the scale of the mechanism design micrometer, millimeter, or meter. For all the nine categories further elaboration and examples are shown.

Only in a very limited amount of the papers found concerning compliant transmission systems, the energy

efficiency analysis is discussed. Even if the efficiency is obtained, it is often not described to be optimized. It is found that when the objective of the optimization of the mechanism is energy efficiency, this usually leads to high-efficiency mechanisms. However, most mechanisms described in this paper are optimized for displacement or force characteristics, showing lower efficiencies. Metal is identified to be most often used in mechanisms showing high efficiencies. In contrast, mechanisms using multiple materials usually show lower energy efficiency characteristics within the selection of this research.

From the design approach combined with the overview of the performance for the mechanisms, different methods are identified which enhance energy efficiency. These methods include Size optimization, Static balancing, Part reduction, Topology optimization, Dynamical, or none. The methods that showed a significant difference in energy efficiency are: Static balancing, which shows great potential for high-efficiency systems, and Topology optimization, for which only low-efficiency results are found. Thereby, the main contributions to energy loss are identified to be: friction, mostly in planar structures, and strain energy, which is often reduced but not completely canceled out. Static balancing can offer a solution in compensating the strain energy which is needed for deformation, however non-conservative forces such as friction or possibly viscoelastic forces, can not be removed or compensated for.

Many mechanisms found are not optimized in terms of energy efficiency and no analysis of the efficiency is done for the currently existing designs. This gap in literature can be exploited and result in great opportunities for the enhancement of these systems. Future research could include using the identified methods for energy efficiency enhancement and applying these to a broader scope of mechanisms. Besides that, it would be useful to develop standard methods of incorporating these methods in compliant design.

REFERENCES

[1] Larry L. Howell, Spencer P. Magleby, and Brian M. Olsen. *Handbook of Compliant Mechanisms*. 2013.

[2] Davood Farhadi Machekposhti. Compliant transmission mechanisms, 2018.

[3] Sohail Iqbal and Afzaal Malik. A review on MEMS based micro displacement amplification mechanisms. *Sensors and Actuators, A: Physical*, 300:111666, 2019.

[4] Jaroslav Hricko. Compliant Mechanisms for Motion / Force Amplifiers for Robotics. (January), 2020.

[5] Jacob S Lewis, Zahra Barani, Andres Sanchez Magana, and Fariborz Kargar. A review of compliant transmission mechanisms for bio-inspired flapping-wing micro air vehicles. pages 0–31, 2019.

[6] D. Farhadi Machekposhti, N. Tolou, and J. L. Herder. A review on compliant joints and rigid-body constant velocity universal joints toward the design of compliant homokinetic couplings. *Journal of Mechanical Design, Transactions of the ASME*, 137(3), 2015.

[7] Tony Atkins and Marcel Escudier. *A Dictionary of Mechanical Engineering*. 2013.

[8] Sridhar Kota, Joel Hetrick, Zhe Li, and Laxminarayana Saggere. Tailoring unconventional actuators using compliant transmissions: design methods and applications. *IEEE/ASME Transactions on Mechatronics*, 4(4):396–408, 1999.

[9] Juan A Gallego. *Statically Balanced Compliant Mechanisms: Theory and Synthesis*. 2013.

[10] Benliang Zhu, Xianmin Zhang, Hongchuan Zhang, Junwen Liang, Haoyan Zang, Hai Li, and Rixin Wang. Design of compliant mechanisms using continuum topology optimization: A review. *Mechanism and Machine Theory*, 143, 2020.

[11] Just L Herder. Energy-free Systems, 2001.

[12] Boaz L. Rijff and Just L. Herder. An energy approach to the design of single degree of freedom gravity balancers with compliant joints. *Proceedings of the ASME Design Engineering Technical Conference*, 6(PARTS A AND B):137–148, 2011.

[13] Giuseppe Radaelli, Juan A. Gallego, and Just L. Herder. An energy approach to static balancing of systems with torsion stiffness. *Journal of Mechanical Design, Transactions of the ASME*, 133(9):1–8, 2011.

[14] Yanhua Zhou, Fugui Xie, and Xinjun Liu. Optimal design of a main driving mechanism for servo punch press based on performance atlases. *Chinese Journal of Mechanical Engineering (English Edition)*, 26(5):909–917, 2013.

[15] Paulo Flores and Hamid M Lankarani. *Solid Mechanics and Its Applications Contact Force Models for Multibody Dynamics*. Number January. 2016.

[16] Jianwei Lu, Yi Xu, Chen Hu, Alexander F. Vakakis, and Lawrence A. Bergman. 5-DOF dynamic model of vehicle shimmy system with clearance at universal joint in steering handling mechanism. *Shock and Vibration*, 20(5):951–961, 2013.

[17] Yanling Tian, Bijan Shirinzadeh, Dawei Zhang, and Gursel Alici. Development and dynamic modelling of a flexure-based Scott-Russell mechanism for nano-manipulation. *Mechanical Systems and Signal Processing*, 23(3):957–978, 2009.

[18] Jih Lian Ha, Ying Shieh Kung, Sheng Chuen Hu, and Rong Fong Fung. Optimal design of a micro-positioning Scott-Russell mechanism by Taguchi method. *Sensors and Actuators, A: Physical*, 125(2):565–572, 2006.

[19] Mingxiang Ling, Junyi Cao, Minghua Zeng, Jing Lin, and Daniel J. Inman. Enhanced mathematical modeling of the displacement amplification ratio for piezoelectric compliant mechanisms. *Smart Materials and Structures*, 25(7):1–11, 2016.

[20] Mingxiang Ling, Junyi Cao, Zhou Jiang, and Jing Lin. Theoretical modeling of attenuated displacement amplification for multistage compliant mechanism and its application. *Sensors and Actuators, A: Physical*, 249:15–22, 2016.

[21] Larry L. Chu, Joel A. Hetrick, and Yogesh B. Gianchandani. High amplification compliant microtransmissions for rectilinear electrothermal actuators. *Sensors and Actuators, A: Physical*, 97-98:776–783, 2002.

[22] Lei Jie Lai and Zi Na Zhu. Design, modeling and testing of a novel flexure-based displacement amplification mechanism. *Sensors and Actuators, A: Physical*, 266:122–129, 2017.

[23] Xiaoqing Sun and Bintang Yang. A new methodology for developing flexure-hinged displacement amplifiers with micro-vibration suppression for a giant magnetostrictive micro drive system. *Sensors and Actuators, A: Physical*, 263:30–43, 2017.

[24] P. R. Ouyang, W. J. Zhang, and M. M. Gupta. Design of a new compliant mechanical amplifier. *Proceedings of the ASME International Design Engineering Technical Conferences and Computers and Information in Engineering Conference - DETC2005*, 7 A(November 2016):15–24, 2005.

[25] Davood Farhadi MacHekposhti, Just L. Herder, Guy Semon, and Nima Tolou. A Compliant Micro Frequency Quadrupler Transmission Utilizing Singularity. *Journal of Microelectromechanical Systems*, 27(3):506–512, 2018.

[26] Tilok Kumar Das, Bijan Shirinzadeh, Ammar Al-Jodah, Mohammadali Ghafarian, and Joshua Pinskier. A novel compliant piezoelectric actuated symmetric microgripper for the parasitic motion compensation. *Mechanism and Machine Theory*, 155:104069, 2021.

[27] Zhengbao Yang and Jean Zu. High-efficiency compressive-mode energy harvester enhanced by a multi-stage force amplification mechanism. *Energy Conversion and Management*, 88:829–833, 2014.

[28] Martin Tschiersky, Giovanni Berselli, Just L. Herder, Dannis M. Brouwer, and Stefano Stramigioli. PZT-actuated compliant locking device. *Proceedings - 33rd ASPE Annual Meeting*, 70:174–179, 2018.

[29] Yuki Ishii, Thomas Thümmel, and Mikio Horie. Dynamic characteristic of miniature molding pantograph mechanisms for surface mount systems. *Microsystem Technologies*, 11(8-10):991–996, 2005.

[30] Guimin Chen, Yakun Ma, and Jiajie Li. A tensural displacement amplifier employing elliptic-arc flexure hinges. *Sensors and Actuators, A: Physical*, 247:307–315, 2016.

[31] Nilesh D. Mankame and G. K. Ananthasuresh. A compliant transmission mechanism with intermittent contacts for cycle-doubling. *Journal of Mechanical Design, Transactions of the ASME*, 129(1):114–121, 2007.

[32] Philip Johannes Steinbild, Peilin Zhang, Karl-Heinz Modler, Andreas Borowski, Marco Zichner, Niels Modler, and Martin Dannemann. *Usability of a Compliant Deltoid Mechanism as a Motion Transmission in Civil Engineering Machinery*, volume 46. Dresden, 2017.

[33] Jessica R Bronson, Gloria J Wiens, and Irene Fassi. Development of a compliant rotary-to-translational transmission mechanism for a micro-parallel kinematic mechanism. *Proceedings of the ASME 2008 International Design Engineering Technical Conferences & Computers and Information in Engineering Conference*, (352):1–7, 2008.

[34] Frederic H. Giraud, Zhenishbek Zhakypov, and Jamie Paik. Design of Low-Profile Compliant Transmission Mechanisms. *IEEE International Conference on Intelligent Robots and Systems*, pages 2700–2707, 2019.

[35] Sujit Pardeshi, Sachin Kandharkar, and Bhagyesh Deshmukh. Monolithic compliant slider crank mechanism for motion amplification. *Materials Today: Proceedings*, 4(2):1677–1682, 2017.

[36] Adil Han Orta and Cetin Yilmaz. Inertial amplification induced phononic band gaps generated by a compliant axial to rotary motion conversion mechanism. *Journal of Sound and Vibration*, 439:329–343, 2019.

[37] Leon Clark, Bijan Shirinzadeh, Yongmin Zhong, Yanling Tian, and Dawei Zhang. Design and analysis of a compact flexure-based precision pure rotation stage without actuator redundancy. *Mechanism and Machine Theory*, 105:129–144, 2016.

[38] Daniele Giannini, Giacomo Bonaccorsi, and Francesco Braghin. Size optimization of MEMS gyroscopes using substructuring. *European Journal of Mechanics, A/Solids*, 84(June):104045, 2020.

[39] Davood Farhadi Machekposhti, N. Tolou, and J. L. Herder. A statically balanced fully compliant power transmission mechanism between parallel rotational axes. *Mechanism and Machine Theory*, 119:51–60, 2018.

[40] Engin Tanik and Volkan Parlaktaş. Compliant cardan universal joint. *Journal of Mechanical Design, Transactions of the ASME*, 134(2):1–5, 2012.

[41] Çail Merve Tanik, Volkan Parlaktaş, Engin Tanik, and Suat Kadiolu. Steel compliant Cardan universal joint. *Mechanism and Machine Theory*, 92:171–183, 2015.

[42] Volkan Parlaktaş, Engin Tanık, and Çağıl Merve Tanık. On the design of a novel fully compliant spherical four-bar mechanism. *Advances in Mechanical Engineering*, 11(9):1–12, 2019.

[43] D. Rodriguez-Cianca, C. Rodriguez-Guerrero, T. Verstraten, R. Jimenez-Fabian, B. Vanderborght, and D. Lefeber. A Flexible shaft-driven Remote and Torsionally Compliant Actuator (RTCA) for wearable robots. *Mechatronics*, 59(February):178–188, 2019.

[44] Chao Zhang, Claudio Rossi, Wei He, and Julian Colorado. Virtual-work-based optimization design on compliant transmission mechanism for flapping-wing aerial vehicles. *2016 International Conference on Manipulation, Automation and Robotics at Small Scales, MARSS 2016*, (July), 2016.

[45] Charles Kim and Sridhar Kota. Design of a novel compliant transmission for secondary microactuators in disk drives. *Proceedings of the ASME Design Engineering Technical Conference*, 5 A(January 2002):77–83, 2002.

[46] J. K. Schonebaum. The design of a monolithic, compliant, resonant running robot at insect scale. 2019.

[47] Claus B.W. Pedersen and Ashwin A. Seshia. On the optimization of compliant force amplifier mechanisms for surface micromachined resonant accelerometers. *Journal of Micromechanics and Microengineering*, 14(10):1281–1293, 2004.

[48] Muqing Niu, Bintang Yang, Yikun Yang, and Guang Meng. Modelling and parameter design of a 3-DOF compliant platform driven by magnetostrictive actuators. *Precision Engineering*, 66(July):255–268, 2020.

[49] Engin Tanik and Eres Söylemez. Analysis and design of a compliant variable stroke mechanism. *Mechanism and Machine Theory*, 45(10):1385–1394, 2010.

[50] Qi Han, Kaifang Jin, Guimin Chen, and Xiaodong Shao. A novel fully compliant tensural-compresural bistable mechanism. *Sensors and Actuators, A: Physical*, 268:72–82, 2017.

[51] Eurico Esteves Moreira, Burkhard Kuhlmann, Filipe Serra Alves, Rosana Alves Dias, Jorge Cabral, João Gaspar, and Luis Alexandre Rocha. Highly sensitive MEMS frequency modulated accelerometer with small footprint. *Sensors and Actuators, A: Physical*, 307, 2020.

[52] Xin Xie, Majid Bigdeli Karimi, Sanwei Liu, Battushig Myanganbayar, and Carol Livermore. Micro motion amplifiers for compact out-of-plane actuation. *Micromachines*, 9(7):1–12, 2018.

[53] Susan Xiao Ping Su and Henry S. Yang. Analytical modeling and FEM simulations of single-stage microleverage mechanism. *International Journal of Mechanical Sciences*, 44(11):2217–2238, 2002.

[54] Yan Xie, Bo Pan, Xu Pei, and Jingjun Yu. Design of compliant universal joint with linear stiffness. *Proceedings of the ASME Design Engineering Technical Conference*, 5A-2016(October), 2016.

3

Technical paper

Reduction of twist moment by application of pre-stress for compliant curved beam transmission systems

R.F.L. Gerlach, 5173907
Thesis MSc. Mechnical Engineering
PME department, Technical University of Delft

***Abstract*—This paper proposes a concept for an I-profile curved beam compliant transmission system. The application of this system can be as a hip connection within a passive exoskeleton in which it transfers the walking motion from one leg to another. To obtain the desired behavior the torsion stiffness is reduced and the amount of work needed to move the system is minimized, resulting in a reduction of 80%. Thereby, it provides a bending stiffness that is almost ten times larger than the torsional stiffness, offering support during bending and lifting movements. Replacing classical subsystems with compliant mechanisms offers opportunities for parts and weight reduction. A proof of concept prototype is obtained out of PA12 and the behavior is demonstrated in a series of experiments. These experiments are supported by a Finite-element analysis, which is also used to predict the behavior for different materials, geometries and applications.**

***Index Terms*—Compliant Mechanisms, Transmission, Energy efficiency**

I. Introduction

Passive exoskeletons are becoming more popular for application, not only in support but also in the prevention of injuries. A passive back support exoskeleton is an example of recent development, offering support in the prevention of lower back injuries. Like most passive back support systems, it exists out of a torso support system and supports connected to the thighs. The upper and lower body components are connected by a spring system, located at the hips. A schematic representation of the system can be found in Figure 1. The exoskeleton offers support when the angle between the upper and lower body is decreased, compressing the spring resulting in a force, pressing the upper body back into an upright position. One of the challenges of the current design is encountered during walking, as this motion also activates the spring system. This requires an increased energy input from the user. Preferably the walking and bending load cases should be handled differently by the exoskeleton. Adding a transmission system on the hips will allow decoupling of the different load cases. The system should transmit the walking motion from one leg to the other and not activate the hip-spring system, while it should be stiff when both legs move in the same direction. This would result in a system with low energy during walking and sufficient back support. A schematic of the system and the two load cases is presented in Figure 2. From this schematic can be obtained that bending over will result in a bending of the system and walking will create twist in the system. Therefore, the desired behavior can kinetically be achieved by obtaining a low torsional stiffness and high bending stiffness.

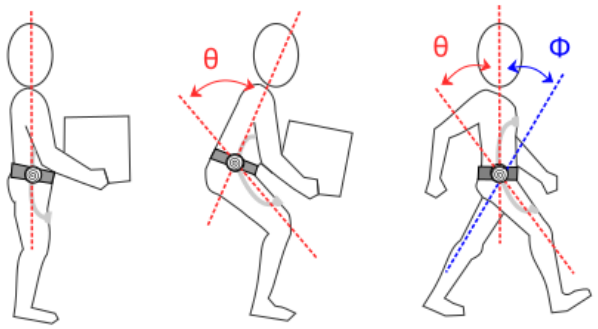

Fig. 1. Schematic representation of the exoskeleton for three different movements: standing, bending, and walking. Variables θ described the angle between the right leg and the upper body, which is the same as the left leg during bending, and ϕ describing the angle between the left leg and the upper body.

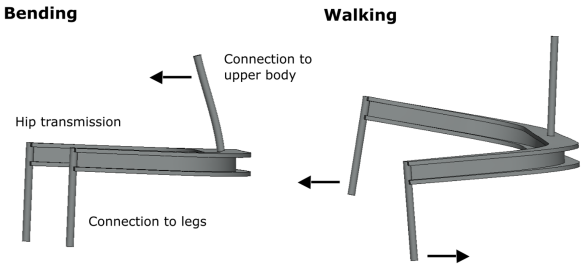

Fig. 2. Concept for a compliant hip transmission for a passive exoskeleton showing the two different load cases: bending, where stiffness is desired, and walking for which compliance is desired.

Different studies have shown methods to alter torsion stiffness. Most of these are directed towards the application in wing structures. Changing the torsion stiffness of a wing is beneficial as the twist of the wing alters the aerodynamics. This twist can then be optimized for different load cases. The research by R. Ajaj et al. [1] shows a concept for an adaptive torsion wing structure. The torsion stiffness can be tuned by changing the area between the front and rear spar webs. The webs are moved towards each other by using internal actuators, resulting in a lower torsion stiffness as the bending stiffness in the desired direction is unaffected. Besides these active systems, multiple concepts exist using pre-stress to obtain the desired behavior. Fundamental designs for a straight beam with reduced torsion stiffness can be found in

[2] and [3] by Lachenal et. al. which show structure with bistable and even neutrally stable behavior. An application of this concept can be found in [4] by Lachenal et al. describing a concept for a zero torsional stiffness twist morphing blade. Another application of prestresses in this context can be found in [5] by M.Schultz which shows a concept for an airfoil-like active bi-stable twisting structures. These concepts contributed to the design as presented in this paper.

To enhance the usability of the system, it should not protrude too far from the user. Creating a curved system will ensure it closely follows the hip shape, decreasing the risk of damaging the surroundings when used. Besides the shape of the system, the size of the hip bracket should be appropriate for the body proportions. Therefore it is chosen to develop a compliant mechanism, as they, among other benefits, offer easy scalability. This scalability can be seen in micro transmission systems, such as presented by Chu et al. in [6]. Furthermore, the weight and complexity are of great importance for the usability and affordability of these systems. Developing a compliant mechanism can result in fewer parts and weight compared to classical systems. The system will be mostly made out of one part and the behavior will be based on its deformation. Studies have shown that using compliant mechanisms results in less friction in the system and therefore less wear as opposed to classical systems. An example of such a system is the compliant transmission mechanism for flapping-wing aerial vehicles as presented by Zhang et al. in [7].

The objective of this paper is to develop a compliant transmission system with reduced torsional stiffness. To obtain this we aim to (i) Apply prestress in a curved structure to manipulate the torsional stiffness, (ii) Decrease the amount of work in the transmission of the walking motion, and (iii) Make an accurate model which can be changed for different use cases. The concept for this paper is based on the application of prestress to obtain bi-stable behavior as is shown in some of the research mentioned above. In contrast to these examples, the principle will be used in a curved structure. The I-profile beam will be curved along the vertical axis. As opposed to previously mentioned examples the prestress in the structure will be applied after manufacturing. This allows for easier manufacturing, as the material is not under tension during assembly, and the possibility to tune the prestress in the system. The amount of work needed to move over the range of motion will be minimized and design will be modeled using FEA software ANSYS allowing to model the different use cases.

This paper will first elucidate on the design and prototyping of the concept in section II. Showing details on the Finite element model as well as manufacturing and assembly. Section III will show the results of the Finite element model in comparison with the results from the experimental setup. This will be followed by a discussion on the results in section IV. The last part of this paper will be spent on a conclusion in section V and future recommendations.

II. Method

A. Design

To create a system that allows for the walking motion and supports the bending motion, a curved I-profile beam will be used. The curvature is important for the fit to the human body. The I-profile has a relatively large bending stiffness which is beneficial in support of the bending load case. The curved beam I-profile geometry has the characteristic of transferring an input rotation applied from one side to the other. By lowering the torsional stiffness of this beam, the transfer of motion could be done with less work put into the system, creating a more efficient transmission. The twist moment will be lowered by trapping energy within the system in the form of pre-stress. By doing so, less energy needs to be added to the system from the outside to move within the desired range of motion.

An overview of the design and the design parameters is given in Figure 7. It is based on two flanges connected by a web, creating the I-profile. In the middle of the curvature, the flange is split into two to create space for the pre-stress. These two strains of the flange which are joint together on both ends will be referred to as the front and rear flanges, their widths are specified by variables w_1 and w_2. The system is pre-stressed by bringing the front and rear flange closer together, reducing the gap. Decreasing the distance s between the front and rear flange creates pressure within the system changing the stable position from a straight configuration to two twisted stable positions.

The mid plane of the beam which coincides with the pre-stress axis is fully constrained. This can, in the final design, be attached to the spine-like structure which connects the upper body to the hip transmission system. The two ends of the system will be connected to leg structures. Therefore the arm to the rotation point can be determined by the Equation 2 and the resulting moment by Equation 1.

$$r = \frac{L}{\sqrt{(dY/m)^2 + 1}} \tag{1}$$

$$M_z = Fy * \left(\frac{L}{\sqrt{(dY/m)^2 + 1}} \right) \tag{2}$$

B. Finite element modelling

To simulate the behavior, the concept design is translated to a finite element model. In this model, the material properties are specified similar to the material properties of the prototype, made out of Polyamide 12. The mesh was made applying the settings for mechanical structures, using a resolution of 3. Six different steps were created in the analysis settings, two steps for pre-stressing the part and four

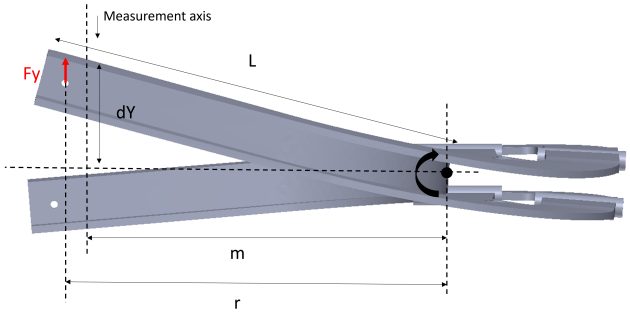

Fig. 3. Side view of the transmission system with geometry parameters for the moment calculation. The input angle ϕ is obtained by displacement dY which is used in the equation.

steps for the movement of the part.

In the solver controls, an iterative solver is selected and the large deflection function is activated to capture the non-linear behavior of the part. Within the nonlinear controls, the Force, Moment, Displacement, and Rotation convergence are removed and the arc length function is activated to find the bi-stable behavior of the part. This is necessary as it is expected that multiple positions will be obtained using the same force. The midplane of the front flanges is fixated, for the bottom as well as the top flange. The load cases differ for each analysis. An overview of the constraints can be seen in Figure 4.

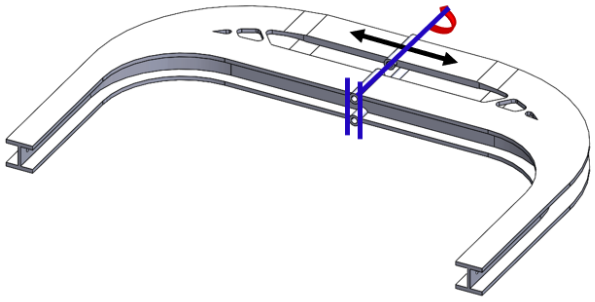

Fig. 4. Model with constraints and loads. The front flange is fully constrained and attached to the back flange. The back flange has the freedom to rotate along the attachment axis, creating freedom for the bi-stable behavior.

1) Flange pre-stress analysis: The pre-stress analysis is done by applying a remote displacement, a translation along the Z-axis, to the center of the back flange during the first two steps. To ensure one of the two stable equilibrium can be found, a perturbation is added in the first step. This is done by adding a rotation of three degrees along the Z-axis.

2) Walking analysis: The movement was modeled by adding a remote displacement, a rotation around the midplane of the front flange, to the ends of the transmission. To simulate the walking motion, only one end of the structure is rotated with the remote displacement. The other end should follow this motion when the force is transmitted properly. The simulated walking angle ranges from -15 up to 15 degrees. The deformed situation for the walking analysis is shown in Figure 5

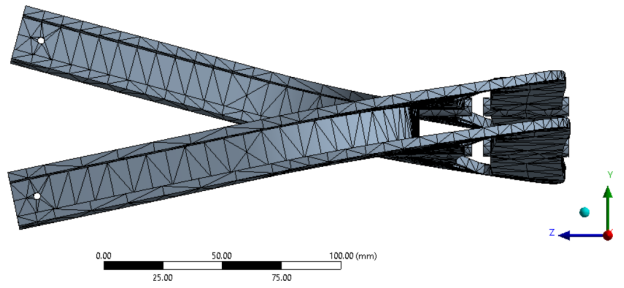

Fig. 5. Deformed geometry at a rotation angle of 15 °for walking analysis

3) Bending analysis: The bending stiffness analysis is done in two steps. The two ends of the structure are rotated around the midpoint, both simultaneously and in the same direction. The two endpoints are first aligned after applying the pre-stress and secondly, the movement is applied. The bending angle is simulated from 0 to -30 degrees. The deformed situation for the bending analysis is shown in Figure 6

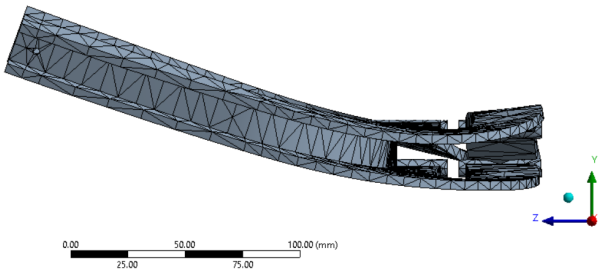

Fig. 6. Deformed geometry at a rotation angle of 30 °for bending analysis.

C. Optimization

The objective of the optimization is to find a configuration that allows for easy walking. The ease of walking can be translated into the amount of effort the user needs to put into the system to get the desired displacement. Therefore, the optimization can be done by finding a minimum in the amount of work needed to move over the range of motion C from -15 up to 15 degrees. The objective function to minimize the amount of work by reviewing the moment and displacement angle can be formulated as stated in Equation 3.

$$min.W = \int_C M d\phi \tag{3}$$

To obtain the desired characteristics for the given design case the stiffness of the mechanism should be tuned. The mechanism can be divided into two parts: the front flange, attached to the web, and the rear flange, contributing to the negative stiffness of the system when pre-stressed. Adding or removing stiffness from one of these can change the twist moment behavior of the mechanism to be linear, bi-stable, or

have a zero stiffness region around the mid position. With only positive stiffness, the behavior will be linear. By adding negative stiffness and balancing it with the positive stiffness, the part will have a zero stiffness region of motion. When more pre-stress is added, the mechanism will become bi-stable. Adding too much will result in very high stresses and might lead to failure.

The width w_1 and thickness t_1 of the flange can be chosen

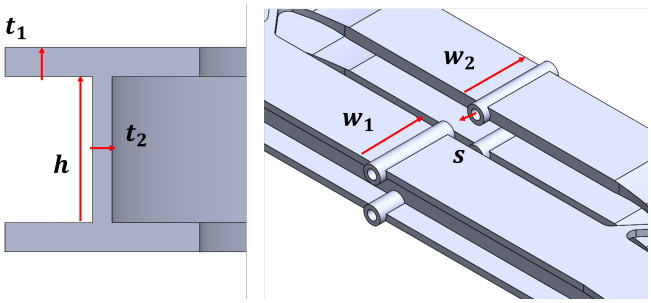

Fig. 7. Schematic of the transmission mechanism design including important design parameters for the behavior of the mechanism. Parameters for the back flange width w_2, web height h, and the pre-stress distance s are used to optimize the design.

according to the requirements for the bending stiffness of the system. Besides that, the desired twist moment should be taken into account. The twist moment can be reduced by adding negative stiffness, but less stiffness will be needed if the structure itself is less stiff. creating lower reaction forces and stresses within the system.

D. Experiments

1) Manufacturing: To verify the FEM model, a scaled prototype was made for experimental testing. This prototype is designed to be half the size of the original design. The prototype was manufactured with Multi Jet Fusion, a Laser Sintering type of additive manufacturing. The part is made out of Polyamide 12 (PA12). Using this material in the print will result in a density of $1.01 g/cm^3$ [8]. The final prototype can be seen in Figure 8.

2) Test-set up: A test setup was made to perform experiments and verify the finite element model. The midplane of the transmission system is fixated and connected to a breadboard. Both ends of the beam are connected to linear guidance systems. The linear guidance holds a vertical slider that is connected to a load cell in the vertical direction. The load cell is connected to the beam with a universal joint. Adding this degree of freedom in the tip allows for tracking of the arc-shaped path of the end of the structure for small angles. An overview of the test setup is given in Figure 9.

To obtain pre-stress within the system, a bolt goes through the flange. By loosening or tightening the nut, the prestress in the flange can be tuned. To obtain the amount of force needed to keep the flange pre-stressed in the desired position a spring was added in the experimental setup between the

Fig. 8. Side view of the prototype fabricated using Multi Jet Fusion from Polyamide 12

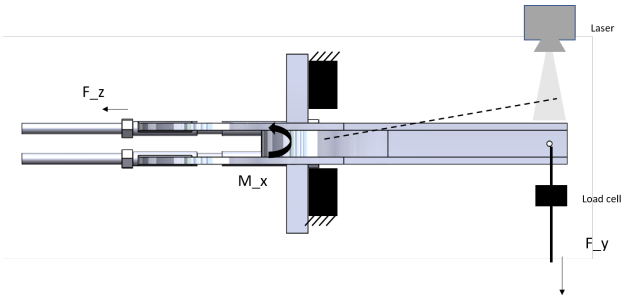

Fig. 9. Schematic of the experimental setup for measuring the bending and torsion stiffness of the system. For the torsion stiffness, only one side of the mechanism is attached to the load cell and moved over a range from -15 °to +15 °. To obtain the bending stiffness, both sides are connected and attached to the load cell. For the bending a range of motion from 0 °to +30 °was used.

back of the flange and the nut. The compression of the spring was measured for different prestress distances. Combined with the spring stiffness, this is translated to a force-displacement curve. Figure 10 shows the test setup used to obtain the force-displacement behavior during the prestressing.

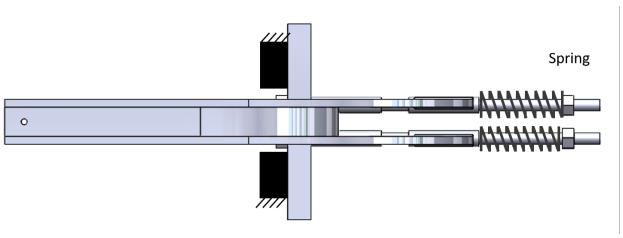

Fig. 10. Schematic of the experimental setup to obtain the force-displacement characteristics of the prestressing mechanism. The force is obtained by measuring the change in length of the compression spring combined with the movement of the back flange.

III. Results

A. Optimization

The width of the back flange w_2 influences the stability of the system. Adding width to the back flange will increase the stiffness, which will contribute to the system as negative stiffness when the back flange is pre-stressed. Figure 11 shows the influence on the behavior when increasing the back flange width. Results from the analysis showed that the web thickness t_2 does not have a significant contribution to the behavior of the mechanism.

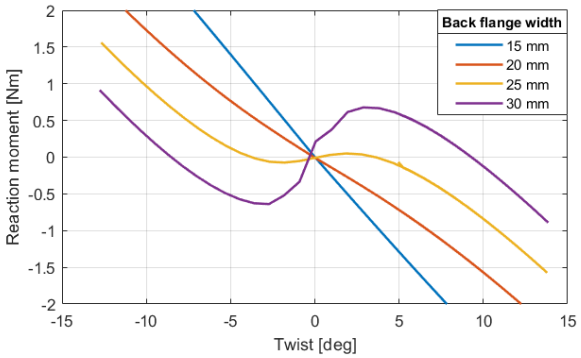

Fig. 11. Twist angle and reaction moment for different widths of the flange w2 ranging from 15 mm up to 30 mm with incremental steps of 5mm.

Increasing the web height h adds stiffness to the system, creating also a stiffer structure during bending. As the web height increases and more positive stiffness is added, the bi-stable behaviour becomes less as can be seen in Figure 12.

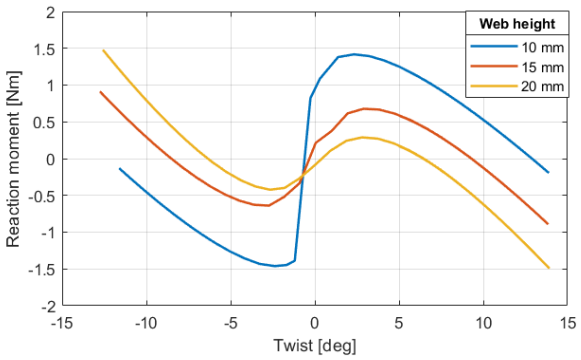

Fig. 12. Twist angle and reaction moment of the mechanism for different web heights, 10 mm, 15 mm, and 20 mm

Besides the geometry of the mechanism, the amount of pre-stress added to the system can be used to obtain the desired characteristics. Figure 13 shows the torsional stiffness for different pre-stress distances. By increasing the pre-stress distance s, more stress is captured within the part, creating more negative stiffness and bi-stable behavior. Making the mechanism more bi-stable decreases the maximum moment needed to rotate within the desired range from 1.7 Nm to 0.9 Nm.

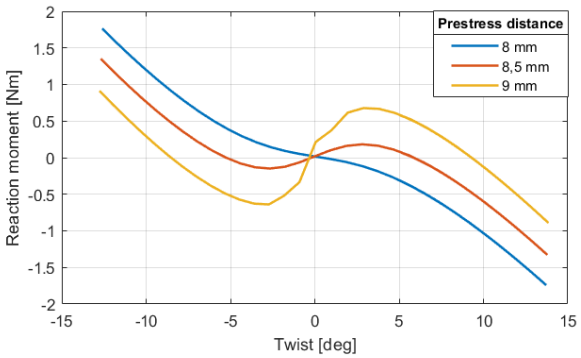

Fig. 13. Twist angle and reaction moment for different amounts of prestressing, defined in the translation distance of 8 mm, 8.5 mm, or 9 mm.

The minimum amount of work configuration was obtained to have a back flange width w_2 of 30 mm and a web height h of 15 mm. The prestress within the mechanism is variable. An overview of the specifications of the final design can be found in Table I.

TABLE I
DIMENSIONS OF THE OPTIMIZED DESIGN

Dimension	Value	Unit
h	15	mm
w	385	mm
w1	30	mm
w2	30	mm
t1	3	mm
t2	2	mm

B. Experiments

1) Pre-stress of flanges: Figure 14 shows the results for the force needed to obtain a desired prestress. Both the experimental and the results of the FEA are given for prestressing distances between 0-3.5 mm. From the graph can be seen that both show linear behavior between 0 and 2.5 mm. For larger prestress distances the graphs deviate more from each other and become less linear. The amount of force needed to keep the flange in the desired position will change during the movement of the system.

2) Torsion stiffness: The torsion stiffness of the structure is obtained by rotating the tips around the midpoint from -15 to 15 degrees. The motion is generated by using a linear guidance system. To obtain the moment, a load cell measures the vertical force necessary to generate the movement. This arm of the force is calculated by obtaining the distance between the force direction and the endpoint, the length of the beam, and correcting for the arc-like path. Multiplying the two creates the results as shown in Figure 15. The experimental results show a hysteresis loop. In both the FEM results and experimental

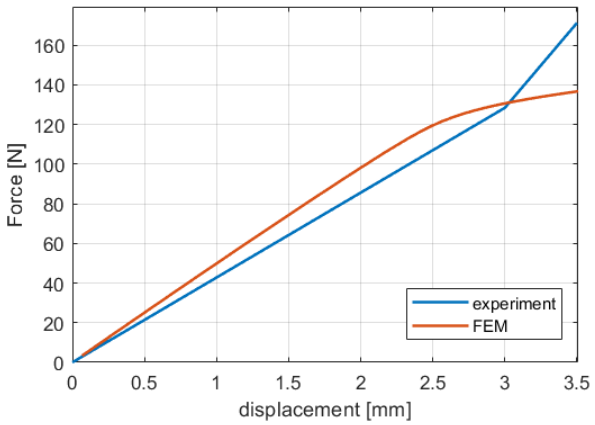

Fig. 14. Pre-stress force and flange displacement in z-axis for the test results and the FEM analysis results.

results the bi-stable behavior is visible.

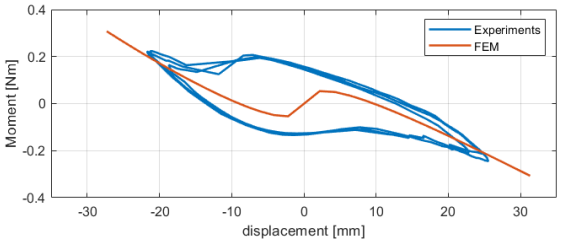

Fig. 15. FEM and test results on the torsion stiffness of the structure for the angles within the walking range -15 to 15 degrees.

3) Bending stiffness: For the system, it is not only important that the work is transmitted during walking, but also that the stiffness is sufficient to support bending. To analyze the bending stiffness a similar setup is used as-is for the torsion stiffness, only both ends are connected to the linear guidance. Both ends are simultaneously rotated from 0 to 20 degrees. Like with the torsion stiffness experiment, the force is obtained in the vertical direction and the moment is calculated correcting for the horizontal movement. The experimental results are averaged to obtain the final curvature. The results for the bending moment for the FEM as well as for the experimental setup are shown in Figure 16.

Combining the results obtained from both the twist moment and the bending moment analysis it can be obtained that for the range between -15 and 15 degrees the twist moment does not become larger than 0.05 Nm. For the bending moment in this range, we see a moment that hits a maximum of 0.5 Nm. Making the bending moment approximately 10 times larger than the twist moment.

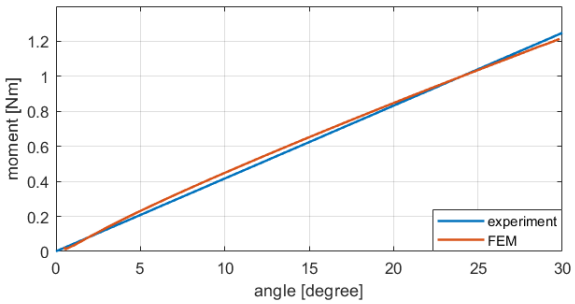

Fig. 16. FEM and test results on the bending moment of the structure for the angles within the bending range 0 to 20 degrees

IV. Discussion

The results obtained in the previous section can be compared to a similar case in which no pre-stress is applied. The comparison between the prestressed and non-prestressed part is given in Figure 17. The maximum torsion stiffness is almost 10 times lower, shifting from 4.6 Nm to 0.5 Nm. When obtaining the amount of work needed for the range of motion, a decrease of 80% can be determined going from 1.13 J to 0.22 J. The obtained design validates the approach and application of pre-stress to reduce the torsion stiffness of a curved I-profile beam. This knowledge can be used and applied in other designs.

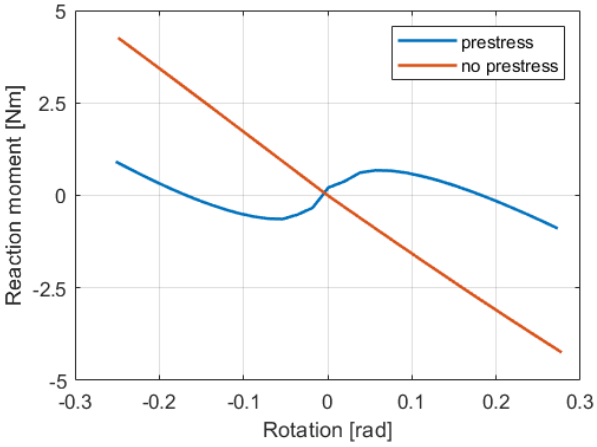

Fig. 17. Twist moment and rotation angle comparison between pre-stressed and non-pre-stressed part obtained from the FEM model for full-size part made from PA12.

For all the obtained results, some of the differences between the FEM and the experiments can be ascribed to the production method, Multi Jet Fusion, which creates a much more isotropic product compared to other additive manufacturing techniques. However, it is not completely isotropic, resulting in different material properties for each axis. This can contribute to a difference in the simulation and experimental results, as the simulation assumes ideally

isotropic behavior.

For small pre-stress displacements, between 0 and 2.5 mm, the results for the experiments and the simulation are comparable. When the system is pushed further towards the limitations in terms of stress, the deviation between the two graphs becomes larger as the behavior becomes less linear. More out-of-plane deflections will occur during this phase which is more susceptible to perturbations. Besides that, the differences in the spring results can be ascribed to the accuracy of the measurements. Which were mostly performed manually, resulting in the presence of human error.

Results for the twist moment show a large hysteresis loop compared to the other measurements. Hysteresis is a phenomenon that is known to apply to products made from polymers, including the prototyping material PA12. To reduce this effect, future designs could be made from metals such as steel or aluminum alloys. Besides that, it can be due to the friction arising between the bolt and the beam when prestressing the structure. The twist motion includes a rotation around this bolt by the back flange. When the system is pre-stressed the back flange is translated along the bolt and fixated with a nut. Between the nut and the flange, there is a force, holding the back flange in the pre-stressed position, but also has friction when the flange wants to rotate. Besides that, the bolt goes through the back flange creating an internal contact area. This contact constraints the out-of-plane movement of the flange, nevertheless, this constraint also brings additional friction to the system during the rotation. Additional experiments were performed including other methods for the prestressing, aiming to lower the friction. The results of these experiments were very comparable to the obtained results as presented in this paper. From this, it can be assumed that the material has the largest influence on the behavior of the system. Further improvements could be obtained by lowering the force needed to apply the pre-stress, as this will lower the friction between the system and the constraints.

The presented mechanism can be applied in various systems requiring transmission of a counter-rotational motion around the same axis. The working principle behind the behavior of the mechanism is mainly captured within the midsection of the curved beam. Therefore, the length of the sides can also be reduced or taken away entirely, while still maintaining the same behavior. An application of the current design could be in humanoid robots or active exoskeleton as a connection between legs and upper body. The objective function can be formulated differently according to the application. This will give a different final design. The mechanism can be tuned to be a bi-stable, neutrally stable, or single stability position system, depending on the desired behavior.

Future research for this design could include the elimination of friction by lowering the force required to pre-stress the mechanism. This force is now relatively high compared to other forces in the system. Lowering the forces that are associated with friction will result in a more efficient system that can be modeled more accurately. Besides that, prototypes produced from other materials, such as metals, could give more information on the long-term behavior and application possibilities of the mechanism.

V. Conclusion

The result of this paper shows (i) That the torsional stiffness can be manipulated by applying pre-stress, (ii) A design with a minimized amount of work, and (iii) An accurate model which can be changed for different use cases.

This paper shows a design for a curved I- profile beam, for which the torsional stiffness is reduced by applying pre-stress. The mechanism exists out of two flanges connected to each other with a web. The flange holds a slit, creating room to apply pre-stress. The pre-stress is applied in the stiffest direction of the I profile by compressing the midplane of the flange together. The amount of prestressing can be changed by changing the constraint translation of the back flange. Changing the pre-stress influences the stability behavior of the mechanism to become neutral or bi-stable. The obtained behavior shows a clear decrease in torsional stiffness when applying this pre-stress.

The amount of work needed to move over the range of motion is decreased by an optimization process controlling three variables: the web height, back flange width, and pre-stress distance. The generated design as presented in the previous sections shows a system that is capable of providing sufficient bending stiffness to support the bending motion. Besides that, the energy for walking is much lower as the amount of work is minimized by changing the torsional stiffness. The result is a bi-stable mechanism. When looking at the obtained results in comparison with a similar I-profile beam without pre-stress, the maximum torsion stiffness is almost 10 times lower. This results in a mechanism that needs five times less energy input to be displaced over the desired range of motion from -15°to +15°. The bending stiffness of the mechanism does not change significantly when adding the pre-stress. Therefore a much higher ratio between the bending moment and twist moment can be obtained, being approximately 10, compared to a value of 2 for non-prestressed systems.

The experimental results are in accordance with the FEM. Verifying the assumptions made during the FEA. The results for the torsion stiffness show the same behavior and the same range of moments as the FEM does, however still have a deviation from the simulated results due to the relatively large contribution of friction and hysteresis in the material, which was not modeled.

REFERENCES

[1] R. M. Ajaj, M. I. Friswell, W. G. Dettmer, G. Allegri, and A. T. Isikveren. Conceptual modeling of an adaptive torsion wing structure. *Collection of Technical Papers - AIAA/ASME/ASCE/AHS/ASC Structures, Structural Dynamics and Materials Conference*, (April), 2011.

[2] X. Lachenal, P. M. Weaver, and S. Daynes. Multi-stable composite twisting structure for morphing applications. *Proceedings of the Royal Society A: Mathematical, Physical and Engineering Sciences*, 468(2141):1230–1251, 2012.

[3] Xavier Lachenal, Stephen Daynes, and Paul M. Weaver. A non-linear stiffness composite twisting I-beam. *Journal of Intelligent Material Systems and Structures*, 25(6):744–754, 2014.

[4] X. Lachenal, S. Daynes, and P. M. Weaver. A zero torsional stiffness twist morphing blade as a wind turbine load alleviation device. *Smart Materials and Structures*, 22(6), 2013.

[5] Marc R. Schultz. A concept for airfoil-like active bistable twisting Structures. *Journal of Intelligent Material Systems and Structures*, 19(2):157–169, 2008.

[6] Larry L. Chu, Joel A. Hetrick, and Yogesh B. Gianchandani. High amplification compliant microtransmissions for rectilinear electrothermal actuators. *Sensors and Actuators, A: Physical*, 97-98:776–783, 2002.

[7] Chao Zhang, Claudio Rossi, Wei He, and Julian Colorado. Virtual-work-based optimization design on compliant transmission mechanism for flapping-wing aerial vehicles. *2016 International Conference on Manipulation, Automation and Robotics at Small Scales, MARSS 2016*, (July), 2016.

[8] Materialise Manufacturing. Datasheets 3D Printing Materials. page 27, 2021.

4

Laevo design case

This section gives additional information about the requirements, realization possibilities, and future design recommendations for the Laevo design case. The current version of the Laevo is not suitable for direct implementation of the hip bracket transmission system. However, future versions which could go towards a spine-like design should be suitable. The system requirements, ass well as the possibilities for the implementation of the system are aimed towards this spine-like design and replace the current smart joints and hip bracket.

4.1. System requirements

An overview of the system requirements is shown in Table 4.1. The most important requirements for this research project are on obtaining the desired behavior combined with the desired shape. A short elaboration on these user and system requirements will follow.

Currently, the amount of support of the Laevo is determined by the smart joints connecting the upper and lower body. Ideally, the function of these smart joints will be integrated within the hip bracket transmission. To obtain similar behavior from the transmission, it must provide a 50 Nm moment for bending angles of approximately 20°. To successfully implement the transmission system, it should not take more energy to walk. The requirement for 3 J per step is based on the desired torsion stiffness combined with the walking angle. To comfortably use the system and decrease the risk of damaging the environment, a maximum design space is defined around the hips of 100 * 100 mm. Laevo uses a standard durability which they guarantee for their product of 2 million steps and 500 thousand forward bends. Other important parameters are the walking angle of 30 degrees, from -15°to 15°. Lastly, the torsion stiffness should ideally be between 1.6 and 5 Nm, this will ensure the leg pads will always be touching the thighs and not lose contact during walking.

4.2. Realisation

To go from the concept to a final product, manufacturing is very important for feasibility. It should be possible to produce the transmission system on a medium to large scale for a relatively low cost. During this project tests were performed with a prototype which was made out of PA12, polyamide, using an additive manufacturing technique. This is not suitable for real-life applications due to two shortcomings: polyamide is not suitable as a material and additive manufacturing is not a suitable manufacturing method for larger-scale production. To ensure the pre-stress does not decrease too much over time, the product can not be made out of an ordinary polymer. Polymers that are loaded show creep over time, decreasing the prestress in the structure. Besides this creep, hysteresis can occur. A good solution to these problems is manufacturing this structure out of metal.

The bi-stable behavior of the system stays the same for different materials, however, the stiffness or

Table 4.1: Requirements for Laevo transmission system for the desired range of motion

Type	Requirement	Specification
User	Support	Must allow to provide support when bending up to 50 Nm in peak
	Energy	Maximum of 3 J per step
	Comfort	100 * 100 mm around the hips
	Durability	Minimal amount of 2.000.000 Steps and 500.000 forward bends
System	Walking angle	Must allow walking angles from -15 up to 15 degrees *
	Torsion moment	Between 1.6 – 5 Nm
	Bending moment	min. 50 Nm at a bending angle of 20 degrees
	Axial stiffness	As high as possible
	CoR	Integrable with remote centre solution
	Stress	Stresses in the material may not lead to plastic deformation or other system failures
	Material	May not be flammable, erode (react with oxygen or water) or shed toxins
Manufacturing	Parts	Less than ten parts, preferably made from one part
	Cost	Less than €250

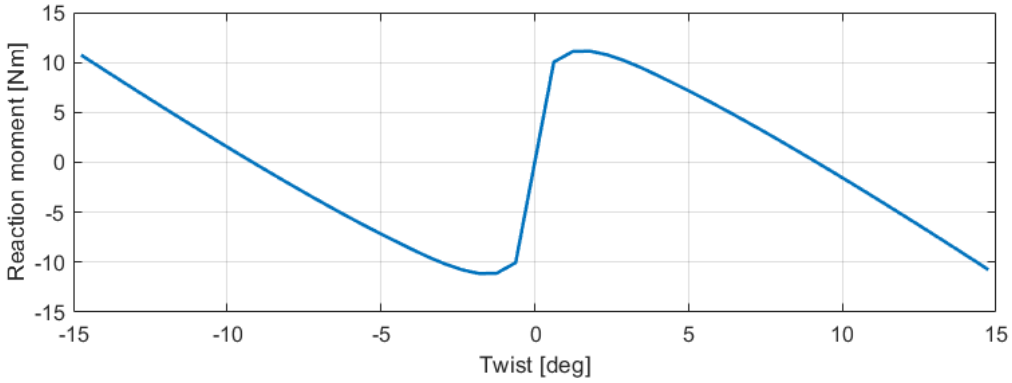

Figure 4.1: Torsional stiffness for the optimized design produced in Aluminum

youngs modulus has a great influence on the magnitude of the deformation in different load cases. The geometry of the design can be changed to balance the stiffness of the material and the stiffness of the beam itself. By changing the thickness and width of the flanges, the stiffness can be tuned. To model the desired deformation for the load cases specified in the requirements, a CAD design was made out of Aluminum alloy. The results are shown in Figure 4.1 and 4.2.

To create the transmission out of the Aluminum alloy, multiple manufacturing techniques are possible. Two options were investigated, Casting, and (laser) cutting & joining. The benefit of casting would be that the part can be created as one and limited assembly steps are needed. However, this will only be profitable for larger batch sizes as the material cost are higher compared to the cutting and joining method. The downside of the cutting and joining method is that the connection between the web and flange influences the behavior and cannot be modeled very accurately. Besides that, multiple assemble steps need to be made to obtain the final part.

The cost of the final product is largely dependent on the manufacturing method and the batch size. The economic batch size of casting is between 1000-1500 units [3], whereas the laser cutting and joining by welding can be feasible for a large range of parts depending on the automation of the process. The price range of the raw material would be approximately 2,12-2,29 EUR/kg [3] for Al-alloys used for casting. As the part will approximately be 400 g, this results in €1,50 in raw material cost.

4.3. Design review

The desired behavior is achieved in a design that fits the requirements for weight and size. An overview of the obtained characteristics is shown in Table 4.2. The maximum bending moment is obtained for 20 °, as was specified in the requirements.

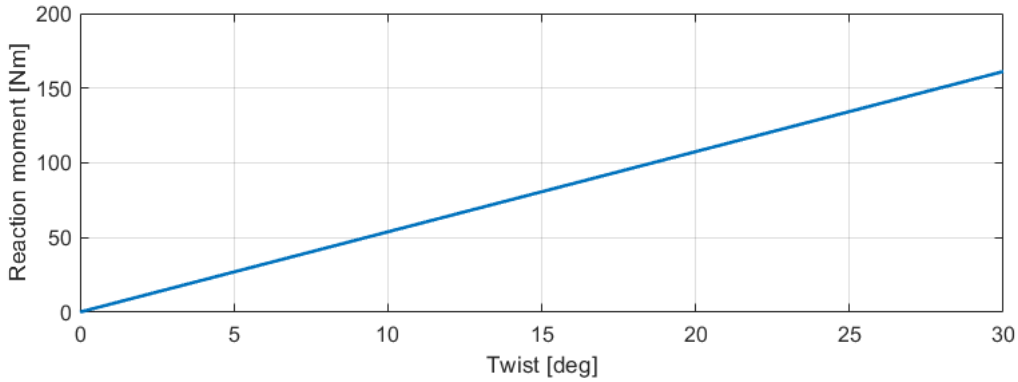

Figure 4.2: Bending stiffness for the optimized design produced in Aluminum

Table 4.2: Obtained results for Laevo design case

	Quantity	**Unit**
Weight	0.4	[kg]
Size	0.36 x 0.24 x 0.023	[m]
Max. bending moment	117	[Nm]
Max. twist moment	11	[Nm]
Energy	2.9	[J]

Future research is necessary for fine-tuning and testing. When the desired dimensions for the hip bracket are known, the structure can be tuned to have the needed stiffness for the different load cases. Besides that, the manufacturing method will need to be tested to obtain the behavior of the final part. Besides that, this will be an important parameter in the overall cost. Lastly, the sustainability of the part is not taken into consideration during this design process. Extensive testing of new prototypes needs to be done to ensure the safety and durability of the system over time. Changing the geometry of the transmission will change the behavior, this can be used for different load cases.

5

Discussion

This report shows a concept for a curved beam transmission system. By changing the system parameters, designs can be obtained to fit different users in terms of size, as the width can be changed or the whole part can be scaled. Besides that, the part can be designed and optimized to have the desired stiffness characteristics, which might change for different use cases. Other applications for this system can be in active exoskeletons or humanoid robotics. It can replace a hip structure and needs less actuation, due to reduced bending forces and easy walking possibilities. Lastly, it can also be applied in less similar systems, where the working principle of this transmission system is desired. In general it can also be used in other machines where there is a desire for a curved system with a low torsional stiffness.

A Finite element model accurately describes the behavior of the mechanism. However, still some differences between the results from the experimental setup and the model are observed. Specifically, the experimental results for the torsional stiffness of the prototype show signs of behavior that is not taken into consideration in the FEM. Firstly, the FEM model is based on the assumption that the material is isotropic. The prototype is made with Multi Jet Fusion, which produces a much more homogeneous part compared to other printing methods, nevertheless, the part will not be completely isotropic. Besides that, the material used, PA12 shows signs of internal damping, resulting in hysteresis. This is a characteristic often seen in polymers and can be averted by using for instance a metal. And finally, the pre-stress force which is needed to obtain the desired behaviour is relatively high compared to other forces working on the system. This results in friction between the constraints and the part, which are also not taken into consideration.

To further enhance the design it would be beneficial to reduce the force needed to apply the pre-stress. One way of doing this would be to decrease the stiffness of the flanges along the pre-stress axis, either by making the flanges thinner or reducing the width of the flange. This will reduce the amount of force needed to obtain the prestress, and have minimal effect on the bending stiffness of the system as the bending direction is orthogonal to the pre-stress direction. To make the behaviour more accurate to the model and more applicable, the part should be made out of metal. This should reduce the amount of hysteresis present in the experimental results. Creating prototypes out of metal will also allow for durability tests, as the part should not show relaxation over time. Some options for manufacturing are mentioned within this report, but a more extensive search and testing should be done.

6

Conclusion

This report shows the development of a compliant curved beam transmission system with reduced torsional stiffness by applying pre-stress. A literature study was done aiming to seek information about the current developments in compliant transmission systems. Secondly, a design is obtained showing the desired behavior, which is explained in the technical paper. Lastly, a design case for Laevo exoskeletons is presented, together with a design that fits their requirements. This section will go into how each of the chapters has contributed to obtaining the final concept.

As an initial investigation on the topic of compliant transmission systems, a literature review was done. In the literature review, a matrix is presented of already available mechanisms divided into nine categories. These categories are based on the motion and scale of the system. To determine the performance of these mechanisms, the efficiency of the found mechanisms was listed or obtained from other results presented in the papers. All mechanisms were then evaluated to determine the method which was used to obtain the efficiency, to identify possible methods which could be applicable in the design process.

The aim of the technical paper is to present a general case of the reduced torsion stiffness curved compliant transmission system design and thereby investigate possible applications besides the one presented in this project. The paper shows a design in which pre-stress is used in the stiffest direction of an I-beam profile curved beam to manipulate the stability and reduce torsional stiffness. The resulting design is made into a prototype from PA12 by using Multi Jet Fusion. Besides that, an accurate FEA model is obtained which can be used as a tool to design the part for different use cases. When changing the stability of the part a different amount of work is needed to move over the desired range of motion. The amount of work is minimized to find the best design for the chosen parameters. A set of experiments performed with the prototype are in accordance with the obtained results from the FEM, which validates the assumptions made in the model.

Initially, the idea and application of this transmission system originate from cooperation with a company Laevo Exoskeletons. Chapter 4 presents the Laevo design case, including the requirements and application in their system. It also holds a design that is fitted to these requirements in terms of design space, the maximum amount of energy, and maximum forces. The design presented is made out of an Aluminum alloy and should fit the average adult. To be able to apply this design in a Laevo exoskeleton some changes still need to be made to go from the Laevo V3 to a spine-like design. Besides that, manufacturing techniques need to be exploited to find a reliable way to produce the number of mechanisms in an economically feasible way.

A

Supplementary material technical paper

This section provides additional material concerning the technical paper. This includes information about the FEM, manufacturing process ass well ass information about the measurement setup and measurement data.

A.1. Finite Element Modelling

Initially, the finite element model was obtained using SolidWorks®. This model showed the resulting stability angle after prestressing. The front of the flange is fully constrained and the back of the flange is pushed forward. To ensure one of the two stable positions would be found, a perturbation is added. Some of the simulation results are shown in Figure A.1.

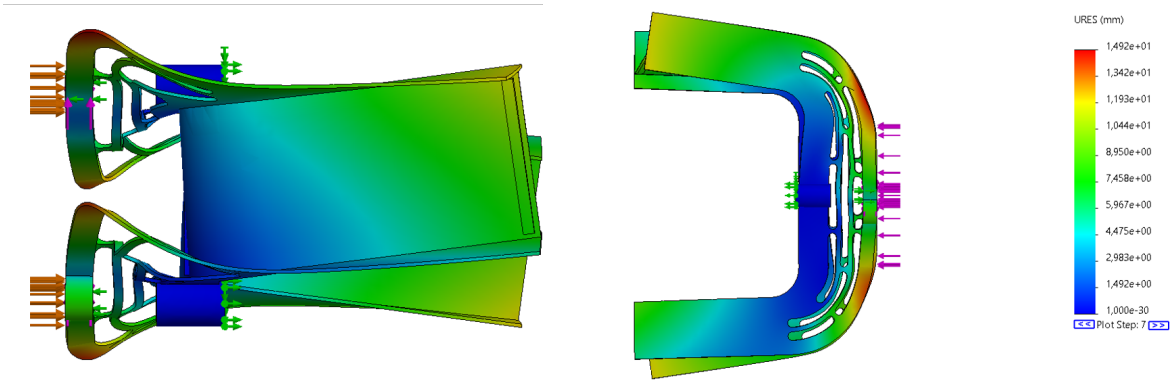

Figure A.1: Absolute displacement results for SolidWorks®model

SolidWorks®started as a computer-aided design program (CAD) but has developed more Finite Element Analysis methods over time. For simple, one-step simulation, this program can be sufficient to obtain a model. The main problem encountered using SolidWorks®was that it is not (yet) possible to define the loading of the mechanism in different steps. This is very important for this mechanism as the prestress should be applied before the displacement for the movement is simulated. Besides that, other limitations were present in the nonlinear analysis settings and the constraints.

For the reasons mentioned above the modelling process was continued in ANSYS®workbench. The final simulation was done in four different steps: 1; prestressing with pertubation, 2; prestressing without perturbation, 3; movement to -15°angle, and 4; movement to +15°angle. The resulting absolute displacement graph is shown in Figure A.2.
Automated optimization of the mechanism can be done by transferring the model into ANSYS APDL.

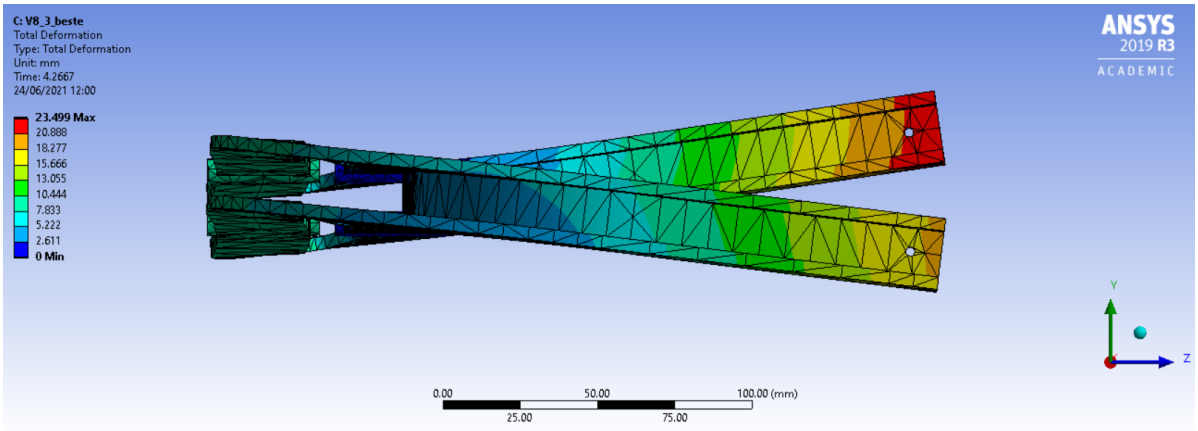

Figure A.2: Absolute displacement results for ANSYS®model

A.2. Prototype

To verify the FEM model, a prototype was made for experimental testing. The prototype was manufactured using Multi Jet Fusion, a Laser Sintering type of additive manufacturing. This method was chosen due to its high resolution, low porosity, and high density compared to other laser Sintering methods. Compared to other additive manufacturing methods in general an advantage is that the print direction has a less significant contribution to the behavior of the material. The mechanical properties are almost similar to injection-molded parts. The part is made out of Polyamide 12 (PA12). Using this material in the print will result in a density of $1.01 g/cm^3$. Other specifications on the material can be found in Figure A.3.

MEASUREMENT	VALUE	STANDARD
Density of parts	1.01 g/cm3	ASTM D792
Tensile Strength, Max Load - XY	48 MPa/6960 psi	ASTM D638
Tensile Strength, Max Load - Z	48 MPa/6960 psi	ASTM D638
Tensile Modulus - XY	1700 MPa/245 ksi	ASTM D638
Tensile Modulus - Z	1800 MPa/260 ksi	ASTM D638
Elongation at Break - XY	20%	ASTM D638
Elongation at Break - Z	15%	ASTM D638
Heat Deflection Temperature - Z	175 °C 95 °C	ASTM D648 @ 0.45 MPa @ 1.82 MPa

Figure A.3: Specifications of the PA12 material when used in multi-jet fusion [7]

To test the measurement setup a part was printed at the university with a standard 3D printer (Prusa i3), using PLA. As expected, this prototype was not suitable for prestressing due to the material properties from the printing process. The stiffness and strength of the material in the layer direction is much higher compared to the direction orthogonal to the layering axis. Therefore the mechanism is not able to handle the pre-stress load as desired and material failure occurs. A picture of this prototype and the material failure is shown in Figure A.4.

Due to the relaxing behavior of polymers, this material is not suitable for application in a product when put under constant pressure. The only way this can be done is when the pre-stress is released when

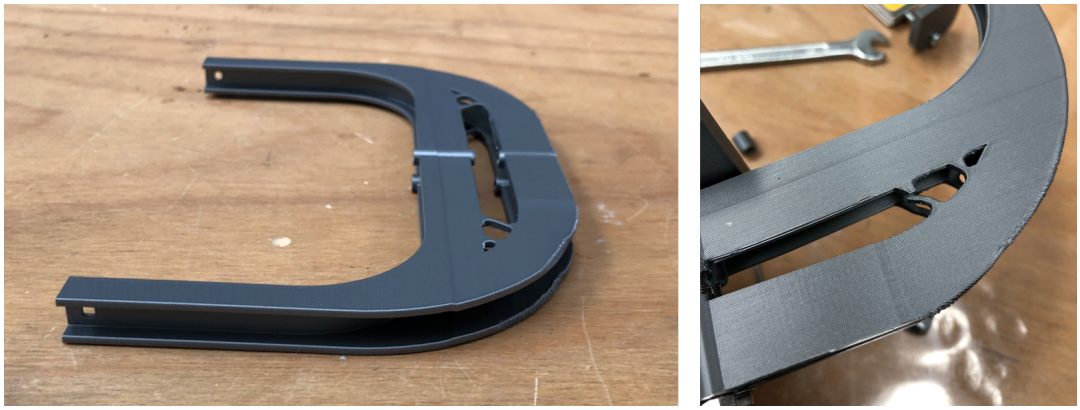

Figure A.4: Prototype from Prusa i3 made from PLA (left) and the material failure (right)

the system is not used and added again when used. As this is not very convenient, the part should preferably be made from metal. For single prototypes, it would be possible to manufacture the part from sheet material that is connected by welding or using special metal glue. As the behavior of the connection will be hard to modal, it is hard to determine if this method will create nice results. For larger batch sizes, it is also economically feasible to make the part by casting [3].

A.3. Measurement setup

This section will elucidate on the enhancements made on the measurement set up before the final setup, as presented in the technical paper, was obtained.

To obtain the force-displacement behavior of the prestress mechanism, a spring is added in series between the nut and the mechanism. Using the change in length of the spring during different pre-stress distances and the spring rate, it will be able to obtain the force. To determine the spring rate, compression experiments were done for two different springs. The results are shown in Figure A.5. As both springs had a force range up to 200 N, spring 2 was chosen due to the larger displacement range. This will create more accurate measurements.

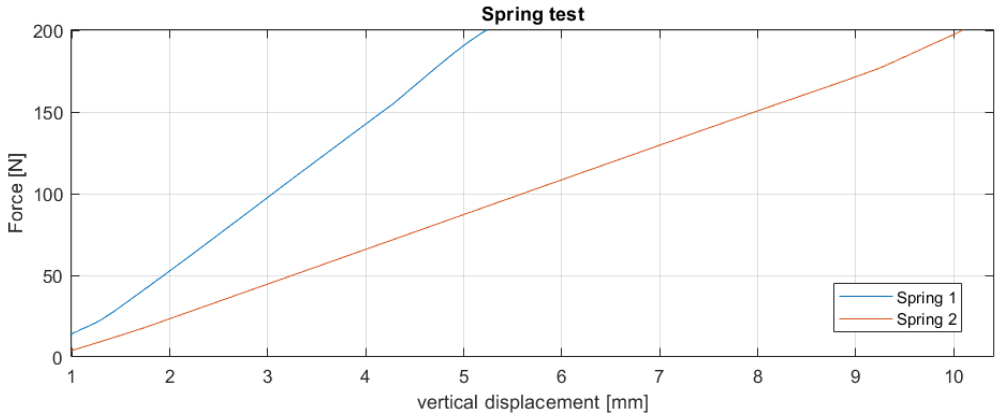

Figure A.5: Experimental spring compression to determine the spring rate of two different springs

Figure A.6 shows an overview of how the measurements for the pre-stress force analysis were performed. One of the problems encountered was the alignment of the spring on the bolt. The radius of the spring was much bigger compared to the M3 thread. To ensure the spring would tilt as least as possible, rings were added around the thread to guide the spring along.

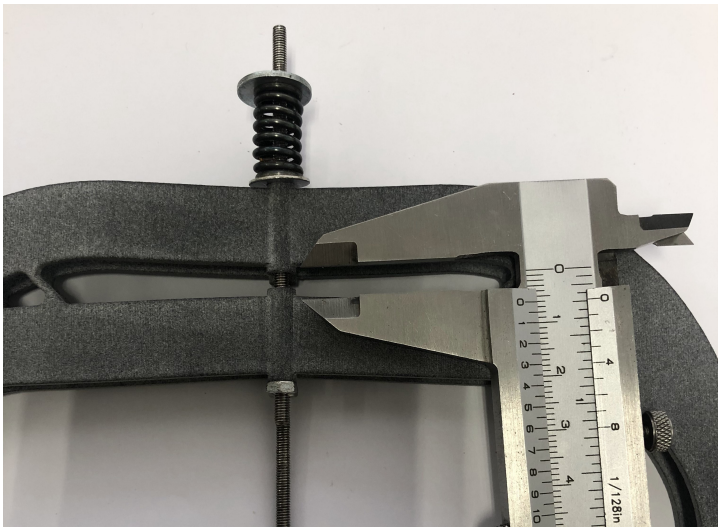

Figure A.6: Experimental setup for measuring prestress force

For the bending and twist tests, a setup was build using a load cell to measure the force and a laser to measure the distance. The load cell is connected to the beam by using a Cardan joint to keep the load cell in a vertical position. The connection between the mechanism and the load cell was made by using a 3D printed connection part and a Cardan joint. The 3D printed connection part should be constrained so it would not rotate when the displacement is applied. As only one connection point was made in the mechanism which could be constrained with a bolt, the connection part was also glued to the mechanism using superglue. The connection is shown in Figure A.7. The other end of the load cell is connected to a linear guidance system which is 3D printed at the university. An overview of the test setup can be seen in Figure A.9.

Figure A.7: 3D printed connection between mechanism and Cardan.

Initially, a horizontal slider was added into the system to create freedom in the tip of the beam for horizontal displacement, as is the case due to the arc-like path. However as these displacements are very small, less than 3 mm, this was unnecessary. Besides that, the additional part brought more play into the system, and the friction was too high for it to move during the twist motion. Therefore this part was removed and the bottom of the load cell was directly connected to the vertical slider. The vertical slider was not performing optimally. When bi-stable behavior was observed it had problems following the displacement due to friction and stick. The experiment was repeated several times, and the resulting data was selected where this did not happen. If the experiments would be repeated, this could be enhanced by making a smoother sliding system.

Figure A.8: Experimental setup for bending with 3D printed beam

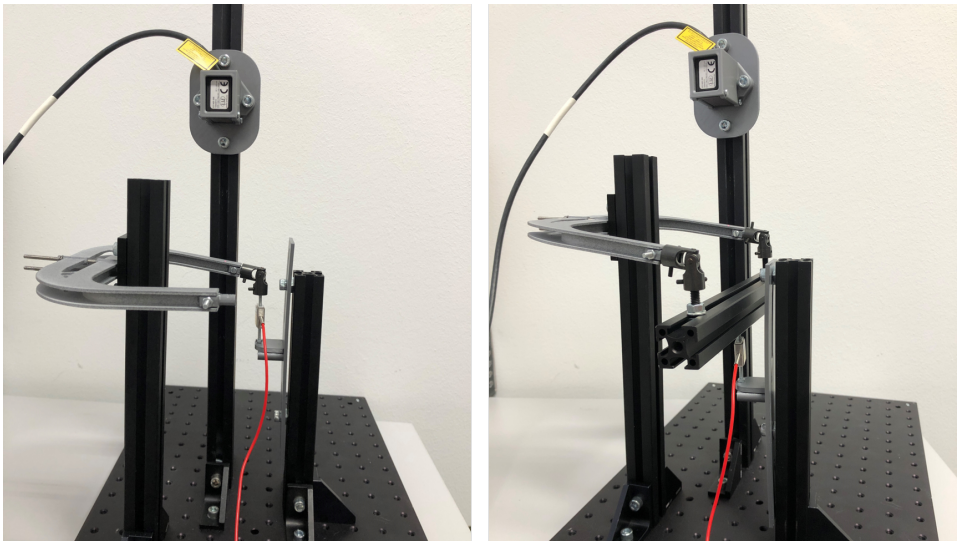

Figure A.9: Experimental setup for measuring: the torsional stiffness (left), and the bending stiffness (right)

For the bending stiffness experiments, the setup was changed to connect the load cell to both tips of the mechanism. Initially, this connection was printed from PLA as can be seen in Figure A.8. However, during testing, the beam turned out not to be stiff enough and showed bending. As this would influence the force-displacement results, a stiffer beam was needed and it was chosen to use an aluminum profile. Besides this connection beam, other parts were replaced with metal parts or printed thicker to ensure the stiffness would not influence the result, for instance, the mid connection plate. An overview of the setup can be seen in Figure A.9. For the bending motion, the friction in the linear guidance system was not a problem and the results were very comparable to the simulation.

As the results for the torsion stiffness showed a large hysteresis loop, further enhancements for the test setup were done. The hypothesis was made that the bolt applying the prestress with the nut contributed to the hysteresis due to friction. Therefore, the new setup did the pre-stressing by pressing two plates together. The back flange was pushed forward by using a ball-slider system to minimize the contact area and give the desired degrees of freedom. An overview of this improved setup can be seen in Figure A.10. As the results were similar to the original obtained results, this setup was not included in the technical paper. The next section will show and elaborate on these results.

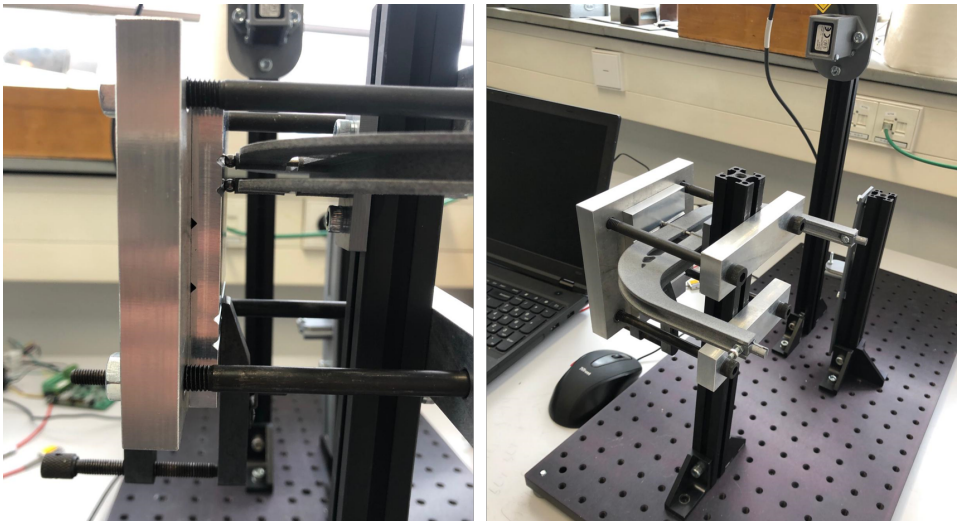

Figure A.10: Improved test setup with a ball- slider system

A.4. Measurement data

The measurement data is shifted and fitted to obtain a smooth graph that can be compared to the simulation data. Both the bending and twist moment data were shifted to compensate for the weight of the attachment between the load cell and the beam. In the bending measurement results, a linear trend was observed as can be seen in Figure A.11. This measurement was therefore fitted with a linear function.

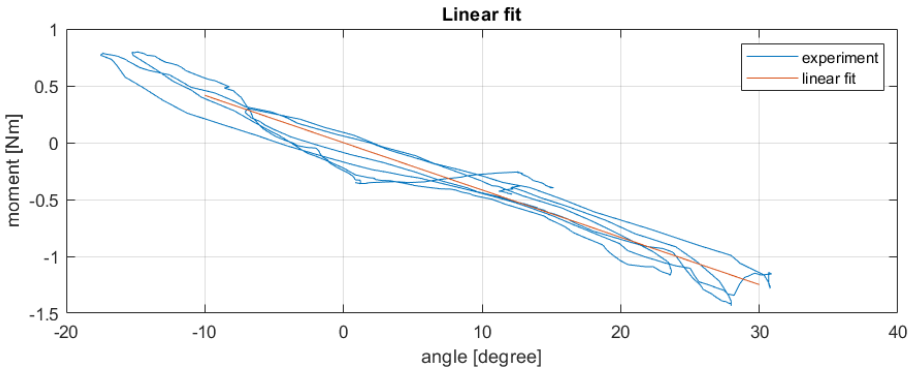

Figure A.11: Bending moment measurement data fitted with a linear curve

For the torsion moment, two different setups were used to examine the influence of friction on the measurement results. For both measurements, the raw data is displayed in Figure A.12. As can be obtained from this figure, the results for both setups were very similar. Therefore the conclusion can be made that the friction in the connection points is not a significant influence in the hysteresis loop. The measurement data for the torsion moment is fitted with a third-degree polynomial, as this function best describes the obtained behavior. The result of the fit is also presented in Figure A.12 .

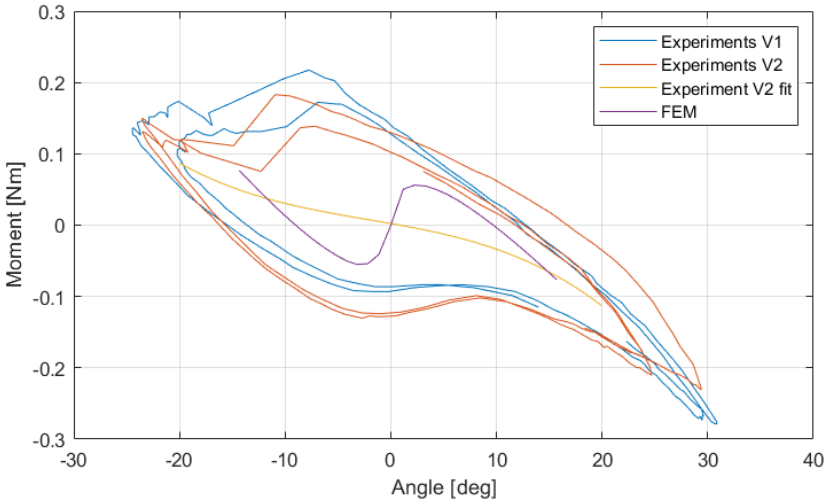

Figure A.12: Twist moment measurement data fitted with a third-order polynomial

B

Concept generation and initial prototyping

To investigate the possibilities for torsion stiffness reduction, multiple prototypes, and simple tests were done. As there are very limited examples available of pre-stress used in compliant mechanisms, different methods were examined on how to apply this in a design. This section shows an overview of the process of these prototypes and also the obtained results.

B.1. Geometry

Multiple ideas for decreasing the torsion moment in the structure were investigated by creating simple prototypes out of sheets of polymers and hot glue. The first designs aimed solely at decreasing the torsion moment by changing the geometry. This was done by using different thicknesses for the web and flanges as well as making holes in the web. With these prototypes, some simple measurements were performed as shown in Figure B.1. The results show a small reduction of torsional stiffness in structures with a thinner web.

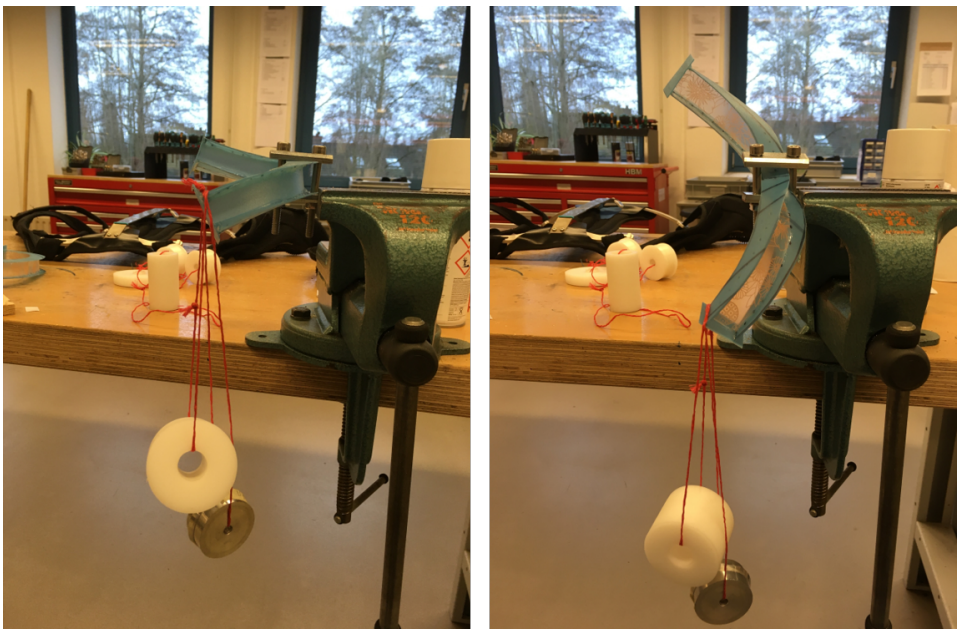

Figure B.1: Initial testing with the first prototypes, single side loading with 205g. left side: thick web, right side: thinner web

B.2. Fixation

A more significant contribution to the results was the fixation of the prototype. The mid fixation of the beam should allow for warping, as well as provide sufficient support for the load cases. Different possibilities are shown in Figure B.2. The most promising being fixation by penetration of the web or flanges, an example is shown in Figure B.2 d.

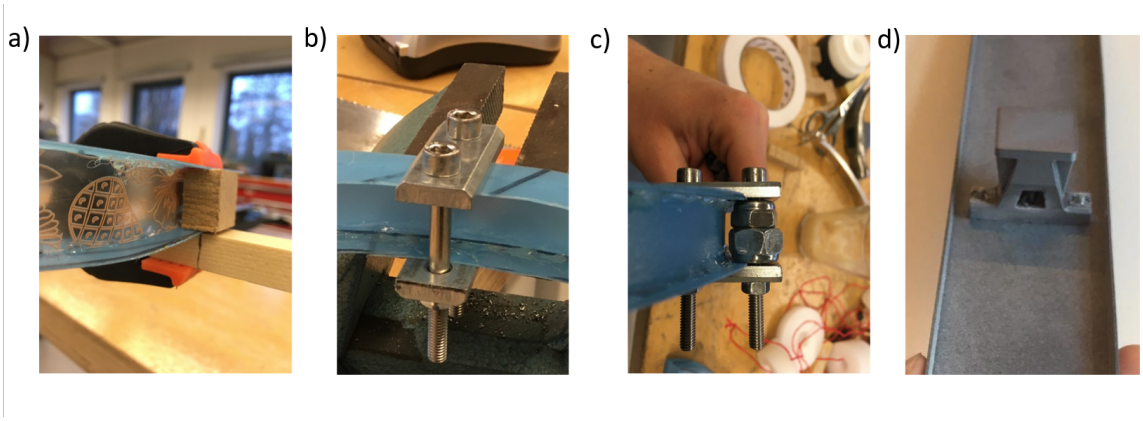

Figure B.2: Possible fixations of the midplane, a) full fixation of midplane, b) box fixation, c) box with fixation of flanges, and d) the fixation of the web

B.3. Pre stress

This method of fixation was implemented and new prototypes were obtained using the principle of pre-stress to lower the torsional stiffness even more. The pre-stress was applied by giving the flanges an initial curvature before fixating them to the web. This approach is similar to what was done by Lachenal et al. in [5]. A prototype combining these two is shown in Figure B.3.

These prototypes did not show the desired behavior. From studying the geometry of the deformed beams it was observed this might be due to the shape of the beam. The pre-curved flanges concept was proven for straight beams, but in a curved configuration, the flanges do not provide tension in the desired direction. Some experiments were done to obtain a flange curvature that does support the transition towards the deformed shape. However, none were found that showed the desired behavior. From the research into the deformed geometry of the curved beam, other concepts were created providing stress in the desired direction. One of the possibilities was creating pre-stress by using springs or elastic bands. Some prototypes for this are shown in Figures B.4 and B.5. However no configuration could be found in which both desired stable positions, left and right twist, were obtained.

Figure B.3: Prototypes using pre-curved flanges to obtain pre-stress in the structure

Figure B.4: Prototypes using elastics to create pre-stress in the structure

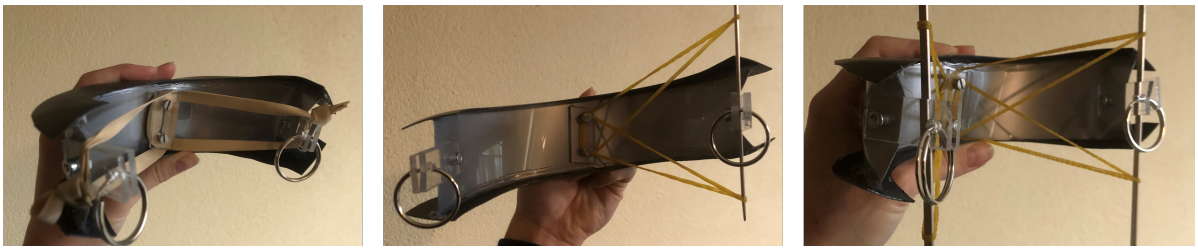

Figure B.5: Prototypes using elastics to create pre stress in the structure

Another option was to create pre-stress in the web instead of the flanges. This possibility was investigated by creating two flanges that could be connected by a spring steel web. This prototype is shown in Figure B.6. No desired behavior was obtained, however, this could be due to the connection between web and prototype, which was difficult between the 3D-printed PLA flange and spring steel web. For manufacturing purposes, it would be easier to have only one material and have a part that can be manufactured as one. Figure B.7 shows one of the fist prototypes in which three stable positions were obtained. It contains two flanges on each side of the web, connected in the middle. The outer flange is longer compared to the inner flange and is pre-stressed by connecting the two ends. As this concept worked nicely, it can be seen as the base for the final design.

As the concept became more established some additive manufactured prototypes were made. The prototypes exist out of two printed flanges connected by a simple web out of a plastic sheet. The parts are again glued together using a glue gun. Figure B.8 shows a prototype with the flanges printed, which gave the desired behavior. However, in the end, it is desired to have two stable positions instead of three and have more control over the stability of the system. To obtain more continuous behavior of

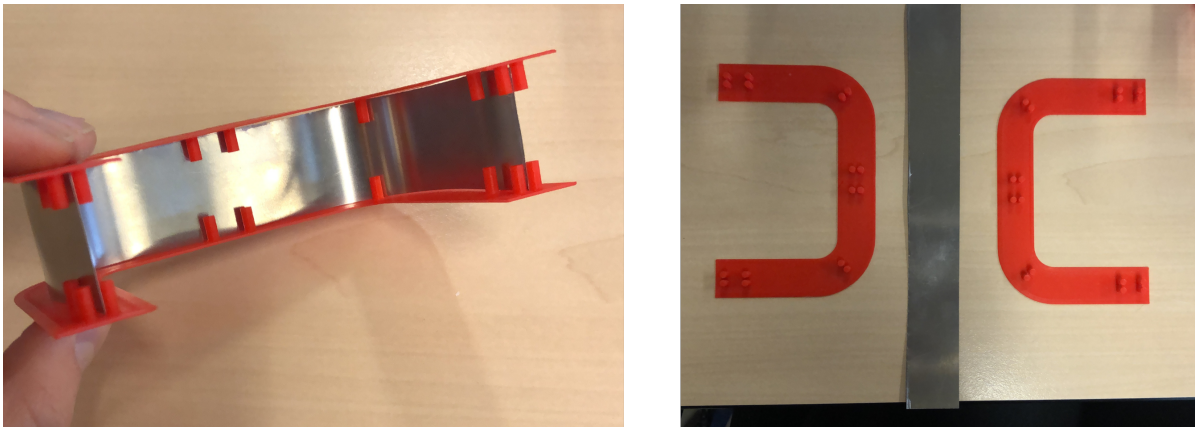

Figure B.6: Prototypes using a spring steel web to create outwards pre stress

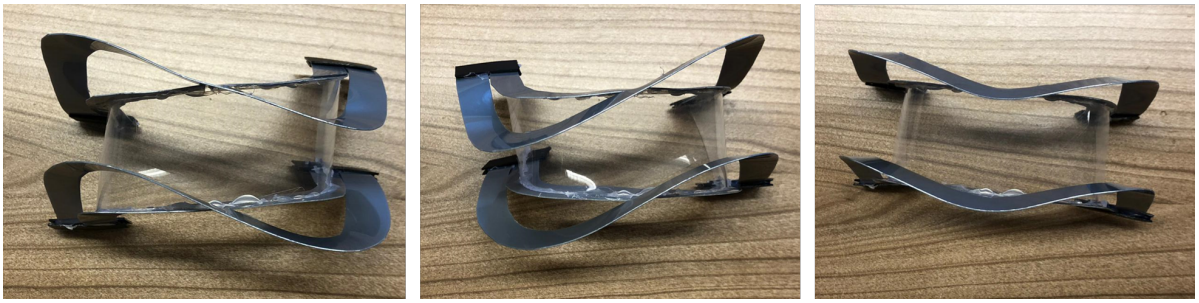

Figure B.7: Prototypes with two connected flanges under pressure creating prestress

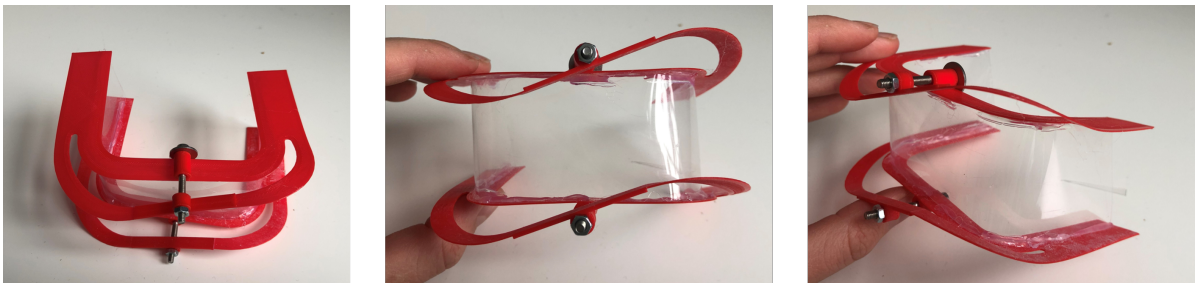

Figure B.8: Prototypes with a printed flange, pre stressed by using a bolt

the flange, the prototype shown in Figure B.9 was made. In this prototype the front and back flange are connected by a series of slits, This prototype showed great potential for a final design and was used as input for the ANSYS®model and FEM analysis.

B.4. Simple experiments

Most prototypes were tested and verified by simply moving over the desired range of motion and doing visual observations on the behavior. For the last series of prototypes, validation was done by adding weights to the system and measuring the in- and output displacement. An overview of the test setup can be seen in Figure B.10. Dark blue indicates the initial position, light blue the position after loading. The Y-displacement is measured as indicated in the figure by measuring the difference in distance to the horizontal. Firstly the measurements were done without pre-stress in the system and secondly with the nuts tightened, adding pre-stress to the system. The results of these tests were in line with the expectations and desired results, as the torsion stiffness was decreased by adding prestress. Figure B.11 shows the results for the measurements of the input displacement and Figure B.12 shows the results for the output displacement. Both were obtained during the same loading instance.

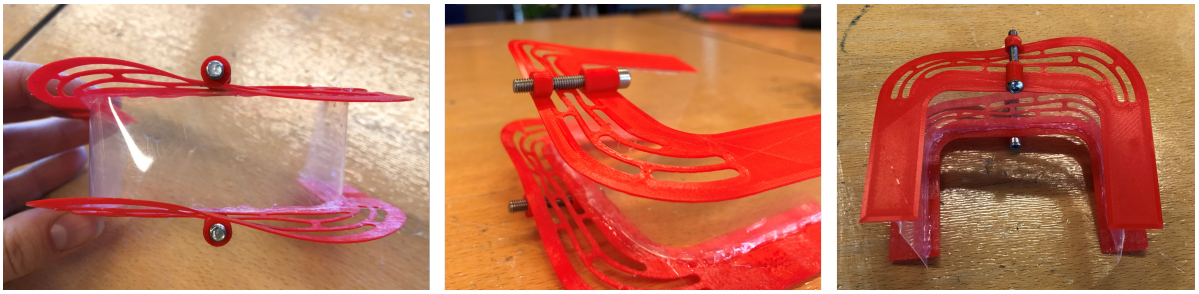

Figure B.9: Prototypes with a slotted connection between the frond and rear flange

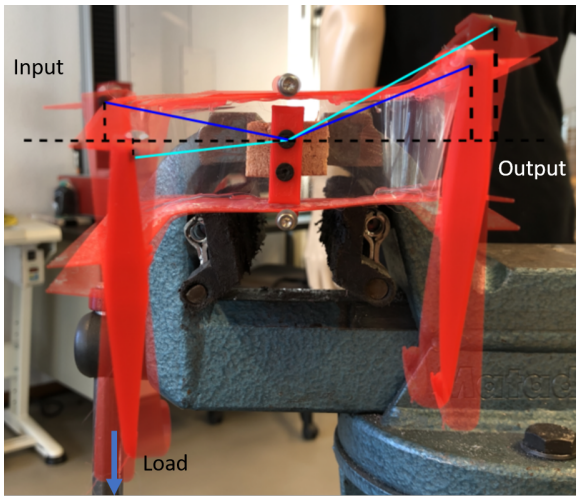

Figure B.10: Overview of test setup for simple testing of initial prototype.

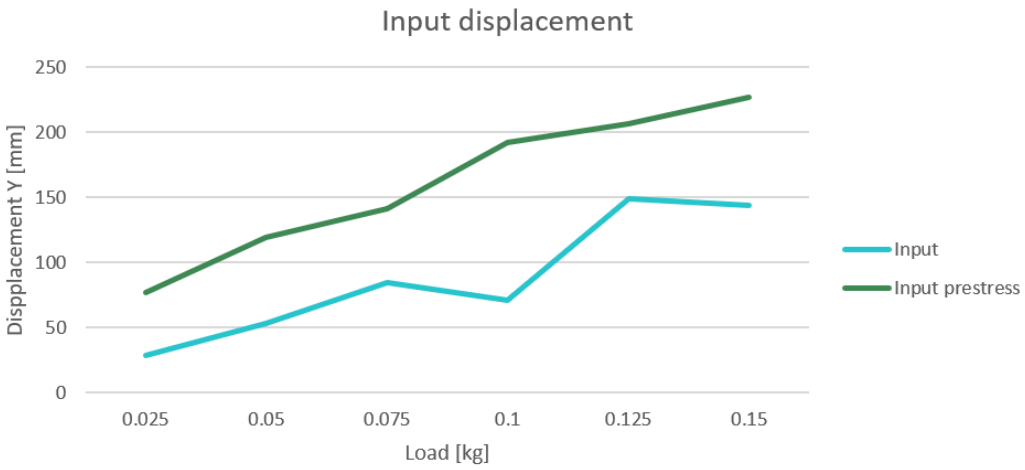

Figure B.11: Overview of test setup for simple testing of initial prototype.

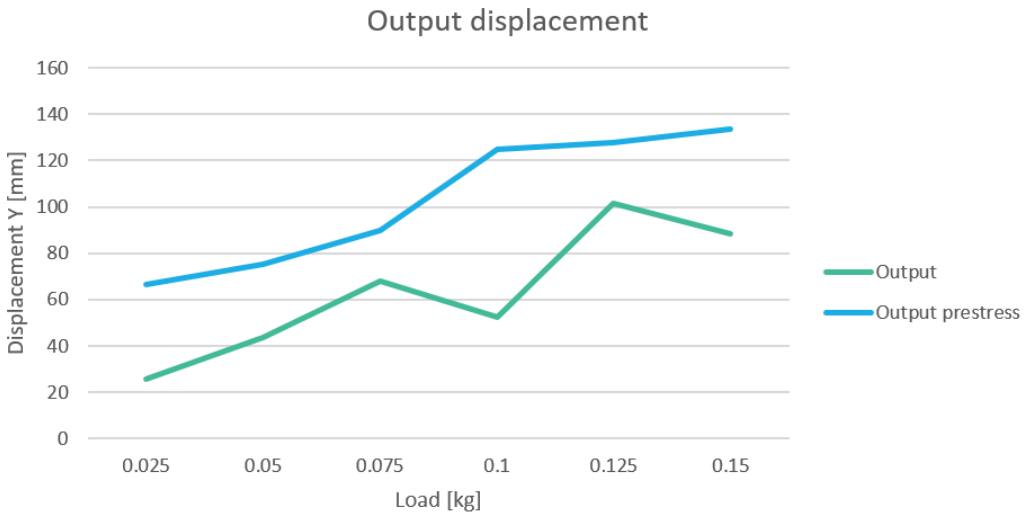

Figure B.12: Overview of test setup for simple testing of initial prototype.

Bibliography

[1] R. M. Ajaj, M. I. Friswell, W. G. Dettmer, G. Allegri, and A. T. Isikveren. Conceptual modeling of an adaptive torsion wing structure. *Collection of Technical Papers - AIAA/ASME/ASCE/AHS/ASC Structures, Structural Dynamics and Materials Conference*, (April), 2011. ISSN 02734508. doi: 10.2514/6.2011-1883.

[2] Frederic H. Giraud, Zhenishbek Zhakypov, and Jamie Paik. Design of Low-Profile Compliant Transmission Mechanisms. *IEEE International Conference on Intelligent Robots and Systems*, pages 2700–2707, 2019. ISSN 21530866. doi: 10.1109/IROS40897.2019.8967701.

[3] Granta Design Limited. CES EduPack. 2019.

[4] X. Lachenal, S. Daynes, and P. M. Weaver. A zero torsional stiffness twist morphing blade as a wind turbine load alleviation device. *Smart Materials and Structures*, 22(6), 2013. ISSN 09641726. doi: 10.1088/0964-1726/22/6/065016.

[5] Xavier Lachenal, Stephen Daynes, and Paul M. Weaver. A non-linear stiffness composite twisting I-beam. *Journal of Intelligent Material Systems and Structures*, 25(6):744–754, 2014. ISSN 1045389X. doi: 10.1177/1045389X13502853.

[6] Davood Farhadi Machekposhti, N. Tolou, and J. L. Herder. A statically balanced fully compliant power transmission mechanism between parallel rotational axes. *Mechanism and Machine Theory*, 119:51–60, 2018. ISSN 0094114X. doi: 10.1016/j.mechmachtheory.2017.08.018.

[7] Materialise Manufacturing. Datasheets 3D Printing Materials. page 27, 2021. URL https://www.materialise.com/system/files/resources/materialise_datasheets_def_file_PA-AF.PDF.

[8] Marc R. Schultz. A concept for airfoil-like active bistable twisting Structures. *Journal of Intelligent Material Systems and Structures*, 19(2):157–169, 2008. ISSN 1045389X. doi: 10.1177/1045389X06073988.

[9] Chao Zhang, Claudio Rossi, Wei He, and Julian Colorado. Virtual-work-based optimization design on compliant transmission mechanism for flapping-wing aerial vehicles. *2016 International Conference on Manipulation, Automation and Robotics at Small Scales, MARSS 2016*, (July), 2016. doi: 10.1109/MARSS.2016.7561715.